ENZYME-IMMOBILIZED HYDROGELS TO CREATE HYPOXIA FOR *IN*

VITRO CANCER CELL CULTURE

A Thesis

Submitted to the Faculty

of

Purdue University

by

Camron Scott Dawes

In Partial Fulfillment of the

Requirements for the Degree

of

Master of Science in Biomedical Engineering

May 2017

Purdue University

Indianapolis, Indiana

THE PURDUE UNIVERSITY GRADUATE SCHOOL
STATEMENT OF THESIS APPROVAL

Dr. Chien-Chi Lin, Chair

> Department of Biomedical Engineering

Dr. Hiroki Yokota

> Department of Biomedical Engineering

Dr. Heiko Konig

> Department of Medicine, IU School of Medicine

Approved by:

> Dr. Edward Berbari
>
> > Head of Departmental Graduate Program

ACKNOWLEDGMENTS

I would like to thank my thesis advisor, Dr. Chien-Chi Lin. This thesis would not have been possible without his patient guidance and the challenging learning environment he provided. He taught me valuable research experience as well as knowledge and critical thinking skills for which I will always be grateful for.

I would also like to thank my advisory committee members, Dr. Heiko Konig and Dr. Hiroki Yokota for their feedback at the culmination of this research. Their time and advice was greatly appreciated.

In addition, I would also like to thank my colleagues; Dr. Tsai-Yu Lin, Dr. Han Shih, Ms. Tanja Green, Mr. John Bragg, Mr. Hung-Yi Liu, and Mr. Matthew Arkenberg for technical assistance and advice. Thanks also to Mrs. Sherry Clemens and Mrs. Summer Layton for assistance and help with the formatting and aesthetics of this thesis. Finally thanks to my family and friends for their continued encouragement and support throughout the last two years.

TABLE OF CONTENTS

LIST OF TABLES

LIST OF FIGURES

LIST OF ABBREVIATIONS

PEG	Poly(ethylene glycol)
PEGDA	Poly(ethylene glycol)-diacrylate
LAP	Lithium Aryl Phosphonate
Acryl-PEG-SVA	Acrylate-PEG-Succinimidyl valerate
O_2	Oxygen
H_2O_2	Hydrogen Peroxide
$CoCl_2$	Cobalt Chloride
TNBSA	2,4,6-Trinitrobenzene Sulfonic Acid
GOX	Glucose Oxidase
CAT	Catalase
GOX_{PEGA}	Glucose Oxidase modified with Acryl-PEG-SVA
LAC	Laccase
FA	Ferulic Acid
BOX	Bilirubin Oxidase
BN	Bilirubin
BTBN	Bis(Tauro)-Bilirubin
RCSB	Research Collaboratory for Structural Bioinformatics
PDB	Protein Data Bank
FBS	Fetal Bovine Serum
RPMI	Roswell Park Memorial Institute Medium
DPBS	Dulbecco's Phosphate-Buffered Saline
DMEM	Dulbecco's Modified Eagle's Medium
AML	Acute Myeloid Leukemia
HCC	Hepatocellular Carcinoma Cells
HIF	Hypoxia Inducible Factor

CA9	Carbonic Anhydrase 9
LOX	Lysyl Oxidase
ANOVA	Analysis of Variance
SEM	Standard Error of the Mean
n	Number of Replicates
$<$	Less Than
$\leq$	Less Than or Equal to
$>$	Greater Than
$\geq$	Greater Than or Equal to
$\pm$	Plus or Minus
$=$	Is equal to
$\approx$	Is approximately
$\cong$	Corresponds to
∂	Partial Derivative
Δ	Change in Quantity

LIST OF NOMENCLATURE

Symbol	Unit	Description
V_{max}	mM·min^{-1}	Maximum enzyme reaction velocity.
V_o	mM·min^{-1}	Enzyme reaction velocity.
K_m	mM	Substrate conc. at which half of V_{max} is reached.
[S]	mM	Substrate concentration.
$[S]_i$	mM	Initial substrate concentration.

ABSTRACT

Dawes, Camron Scott. M.S.B.M.E., Purdue University, May 2017. Enzyme-Immobilized Hydrogels to Create Hypoxia for *In Vitro* Cancer Cell Culture. Major Professor: Chien-Chi Lin.

Hypoxia is a critical condition governing many aspects of cellular fate processes. The most common practice in hypoxic cell culture is to maintain cells in an incubator with controlled gas inlet (i.e., hypoxic chamber). This thesis describes the design and characterization of enzyme-immobilized hydrogels to create solution hypoxia under ambient conditions for *in vitro* cancer cell culture. The first objective of this thesis was to modify glucose oxidase (GOX) for copolymerization with poly(ethylene glycol)-diacrylate (PEGDA) to form GOX-immobilized PEG-based hydrogels. The effect of soluble GOX or acrylated GOX on sustaining hypoxia was evaluated under ambient air condition (i.e., with constant oxygen diffusion from the air-liquid interface). The second objective of this thesis was to use the GOX-immobilized hydrogel system to create hypoxia for *in vitro* culture of cancer cells, including Molm14 (acute myeloid leukemia (AML) cell line) and Huh7 (hepatocarcinoma cell (HCC) line). Under ambient air conditions required for cell culture, the GOX-immobilized hydrogels were able to establish and sustain *in vitro* hypoxic conditions ($<5\%$ O_2) for 6 to 24 hours. Additionally, cell viability and the expression of hypoxia associated genes, including carbonic anhydrase 9 (CA9) and lysyl oxidase (LOX), were evaluated in the presence of GOX-immobilized hydrogels. The third objective of this thesis was to establish hypoxic gradients using the enzyme immobilized hydrogels, which were placed in reservoirs of a commercially available channel slide. The combination of the devices geometry and the enzyme-immobilized hydrogel that served as an O_2 sink permitted the generation of an O_2-concentration gradient within the channel connecting the two reservoirs.

1. INTRODUCTION

1.1 Physiological Hypoxia

Hypoxia, the lack of adequate oxygen (O_2) supply in cells and tissues, is a physiological condition of many healthy and diseased tissues in the body. For example, O_2 concentration is around 20% in the lungs; $\sim$13% in the alveoli; $\sim$5% in the circulation system and the bone marrow; and below 5% in multicellular tissues [1, 2]. Hypoxia is implicated in both normal physiological events and pathological conditions, including ischemia, tumors, and inflamed tissues. As such, O_2 concentration should be considered as a critical experimental condition when performing *in vitro* cell studies [1, 3–5]. Hypoxia stabilizes the expression of hypoxia inducible factors (HIFs) [3], which are heterodimeric transcription factors that regulate many downstream genes and cell fate processes [3, 5], including proliferation, metabolism, apoptosis, stress response, angiogenesis, and migration. Hypoxia is also a key factor regulating tumor growth and drug resistance [2, 4–6].

1.2 Devices to Induce Hypoxia for Cell Culture

The gold standard to induce hypoxia ($[O_2] <$ 5%) for *in vitro* cell culture is through using a cell culture chamber with controlled gas supplies (i.e., hypoxic chamber). However, the time needed to reach equilibrium of O_2 partial pressure between the chamber atmosphere and the culture medium could take several hours [7]. Another challenge of using a hypoxic chamber is that O_2 diffusion from the air to the cell culture media occurs rapidly once the culture plates are removed from the hypoxic chamber. Unfortunately, studies have shown that even brief exposure of some cells to ambient air would cause drastic changes in certain hypoxia-related gene expression [8]. For this reason, a glovebox is required if one wishes to maintain hypoxia throughout

the experiment. The high front-end cost and dedicated space required for a hypoxic chamber system also limit its implementation to selected laboratories. In addition, it is challenging to perform real-time imaging or other instrument-based live cell assays under hypoxia even with the use of a glovebox. Furthermore, one hypoxic chamber system can only provide one fixed O_2 tension for one experiment, which significantly hinders the progress of scientific discovery related to varied O_2 tensions (e.g., hypoxia gradient, multiplex hypoxic drug testing, etc.).

Another method to induce hypoxia for cell culture is through introducing pre-equilibrated media with lower O_2 tension into the cell culture vessels, such as biore-actors or microfluidic devices. Bioreactors are the standard operation for scale-up production of cells or biological products but not ideal for mechanistic studies of hypoxia-induced cellular response. On the other hand, a microfluidic culture system permits real-time imaging of hypoxic cell culture and allows creation of complex hy-poxia patterns within the confined microenvironment. For example, Peng et al. used chemical scavengers to reduce aqueous O_2 content within a patterned array of cells in wells of a microfluidic device with geometry matching that of a 96-well plate [9]. This method is beneficial in that multiple O_2 profiles can be developed rapidly through pre-equilibrated media in different wells of a single device. However, setting up mi-crofluidic cell culture requires special instruments and project-specific microfluidic design. The applicability of such system in higher or enhanced-throughput analysis is also limited (e.g., drug screening and testing under various hypoxic conditions). It is also not an easy task to integrate microfluidic system with three-dimensional (3D) cell cultures.

1.3 Hypoxia induced by enzymatic reactions

O_2-consuming enzymatic reactions are being developed as an alternative route to the aforementioned methods. The most notable example is the use of glucose oxidase (GOX) and catalase (CAT) [10,11]. In this system, GOX oxidizes β-D-glucose while

consuming O_2 to produce gluconic acid and hydrogen peroxide (H_2O_2). CAT is added to reduce the cytotoxic H_2O_2 to one mole of water and a half mole of O_2 (Figure 1.1).

$$\beta\text{-D-Glucose} + H_2O + O_2 \xrightarrow{\text{GOX}} \text{Gluconic Acid} + H_2O_2 \quad \text{(i)}$$

$$H_2O_2 \xrightarrow{\text{CAT}} H_2O + \tfrac{1}{2} O_2 \quad \text{(ii)}$$

$$\beta\text{-D-Glucose} + \tfrac{1}{2} O_2 \xrightarrow{\text{GOX + CAT}} \text{Gluconic Acid} \quad \text{(iii)}$$
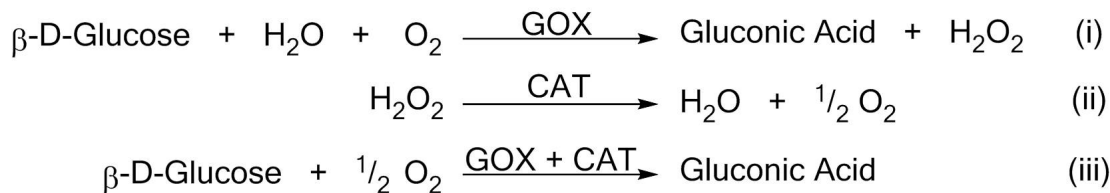
Fig. 1.1. Enzymatic reactions of GOX (i), CAT (ii), and GOX/CAT (iii).

This system has been applied to induce hypoxia in solutions, microfluidic chambers, etc. [12–20]. The use of GOX/CAT is beneficial in that the system provides a rapid onset of hypoxia (usually within a few minutes) [12–20]. One drawback to any GOX system, however, is the production of hydrogen peroxide (H_2O_2), a reactive oxygen species (ROS) [21] whose accumulation would not only cause undesired cellular response but also inactivate both GOX and CAT [22–25]. Thus far, the applications of GOX/CAT system have been focused on glucose sensing and pH-induced responses [26]. For example, Choi et al. prepared GOX-immobilized poly(ethylene glycol) (PEG) hydrogels and studied the effect of gel compositions on immobilized enzyme activity. Although the production of H_2O_2 was quantified to evaluate kinetics of the immobilized enzyme kinetics, O_2 contents were not monitored [27]. Some recent work has started to explore the ability of GOX/CAT reactions to induce hypoxia for in vitro cell culture [12–15, 17–20]. The GOX/CAT system has also been adapted to 3D printed inserts [20] where GOX and CAT were coated on printed disks and the degrees of solution hypoxia were controlled by the distance between the enzyme-immobilized disks and the solution in the culture plate. In that design, hypoxia conditions (between 0 and $\sim$12% O_2) were maintained for up to 5 hours and the system was used to induce hypoxic response in peritoneal macrophages.

Other enzymes (e.g., laccase) have also been used to create hypoxia [28–30]. In the laccase system, a fixed amount of substrate (i.e., ferulic acid, FA) was immobilized to

a polymer backbone. The FA-immobilized polymer was then crosslinked by laccase-mediated enzymatic reaction, which also consumes O_2. Recently, Lewis *textitetal.* extended the timespan of laccase-induced hypoxia by limiting the diffusion of O_2 into the FA-crosslinked hydrogel. Together with the enzymatic O_2 depletion, the system was successfully used to study the impact of hypoxia on sarcoma cell invasion and migration [31].

1.4 Methods of Enzyme Immobilization

Enzyme immobilization can be accomplished through physical adsorption/entrapment, electrostatic forces, covalent crosslinking, or biomolecule binding. With any method, it is important to retain a degree of affinity for the enzyme and its substrate while maintaining enzymatic activity. Additionally it is important for immobilization methods to be efficient such that the effective concentration of enzyme is sufficient to produce a desired level of enzymatic product. If immobilized enzymes are used for cell culture it is also ideal to use chemicals that are mild, thermostable, and biocompatible for immobilization so as to not affect cytocompatibility. PEG provides a polymeric backbone for forming cytocompatible hydrogels. PEG itself is inert and has no cellular recognition sites; it is easily modifiable with functional groups to provide crosslinking between monomer chains. Several common crosslinking schemes for PEG-based hydrogels are shown in Figure 1.2 [32]. These methods can be readily adapted for enzyme immobilization, as long as appropriate functional groups are functionalized on the enzyme surface.
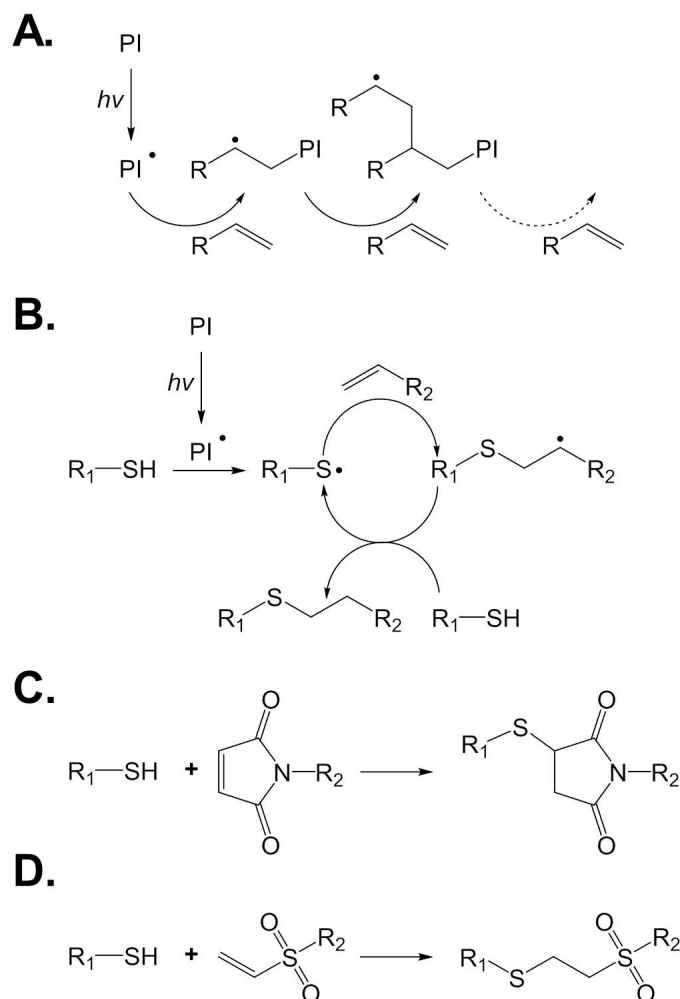
Fig. 1.2. Chemical reactions for hydrogel crosslinking and covalent immobilization of target molecules. (A) Free radical mediated chain-growth photopolymerization. (B) Step-growth thiol-ene polymerization. (C) Base catalyzed thiol-maleimide click polymerization. (D) Thiol-vinyl sulfone polymerization. (R, R_1, R_2 = polymer functional groups or target molecule moieties for immobilization; PI = photoinitiator; hv = light source).

Both chain-growth (Figure 1.2A) and step-growth polymerization (Figure 1.2B) are gelation schemes that require a photoinitiator and a light source to generate free radicals for initiating polymerization. Immobilization of enzymes in hydrogels can be accomplished by functionalizing the enzymes with vinyl containing moieties (e.g. acrylate or methacrylate). Subsequently, the acrylated or methacrylated en-

zyme can be co-polymerized within chain-growth polymerized hydrogels. Another class of commonly used gelation method is Michael-type bioorthogonal click chemistry, which does not rely on light or photoinitiator (Figure 1.2C & D). Michael-type chemistries involve the nucleophilic conjugation of an electron donor (called Michael-donors) with an electrophilic C=C double bond neighboring a carbonyl group (called Michael-acceptors) [33]. Often, thiol groups (-SH) are used as Michael-donors since they are easily oxidized and can be found in proteins and peptides in the form of cysteine residues. Most proteins however only have a few thiol groups that are surface accessible for chemical immobilization. To increase protein immobilization efficiency, chemical modification (e.g., thiolation with Trauts reagent) is necessary to afford additional thiol groups on the proteins [34].

1.5   Implications of Hypoxia Gradients in Cancer Cell Culture

Hypoxia is commonly implicated with tumor physiology. During tumor development, cells rapidly proliferate and form irregular vasculature and structural geometries. This irregular vasculature combined with cellular O_2 consumption and the diffusion limit of O_2 in tissue results in a radial gradient of O_2 concentration to exist within tumors. Often, lowest O_2 concentration is found in the tumor core and increases as moving outward towards the periphery. It is also possible tumor growth to occur next to arteries. O_2 also decreases within the tumor the further away from the artery one inspects. Tumors with sections of tissue having less than $\sim 1.4\%$ O_2 are correlated to increased risk of metastasis, remission, and resistance to radiotherapy treatment [35–38]. Understanding the correlation between tumor growth and hypoxia could lead to better treatment regimens at different stages of cancer physiology. With this goal, Grimes *et al.*, developed and validated a mathematical model to describe the diffusion limit of O_2 within different sized cancer cell spheroids (a tumor like cell model) [39]. They found that the diffusion limit of O_2 within cell spheroids, and by extension tumors, was ~ 230 μm. It could be inferred that if a tumors mass exceeded the radial distance of ~ 230 μm from an artery there was little or no partial pressure

of O_2 at the distal locations from the artery. This assumption could also be made for tumors without close proximity to an artery, where if the tumors radius was larger than $\sim$230 μm, pockets of tissue with no partial pressure of O_2 would develop in the center mass.

Within hypoxic areas with O_2 less than 1.4%, hypoxia inducible factors can induce the expression of matrix remodeling enzymes. One such enzyme is Lysyl oxidase (LOX), which crosslinks lysine or hydroxylysine residues on collagen strands which causes an increase overall ECM stiffness [38, 40, 41]. A stiffer ECM stimulates migration of the tumor cells to invade surrounding tissues. With its correlation to tumor cell metastasis, the expression of LOX is often used as a prognosis indicator [38, 40, 41]. Carbonic Anhydrase IX (CA9), a transmembrane glycoprotein, is also upregulated under hypoxia. CA9 catalyzes the reversible transformation of carbon dioxide to carbonic acid, whose accumulation leads to environment acidification, which is believed to contribute to tumor growth and tissue invasion. Currently CA9 expression is used as a prognostic indicator of intratumoral hypoxia, induced angiogenesis, high cancer relapse rate and low survival [42, 43].

2. OBJECTIVES

2.1 Overview

This thesis presents a simple immobilized enzyme strategy for inducing hypoxia within and surrounding the PEG-based hydrogel for *in vitro* cancer cell culture. The ability of GOX, PEG-acrylate modified GOX (i.e., GOX_{PEGA}), and GOX-immobilized hydrogels to induce solution hypoxia was systematically studied. Furthermore, GOX-immobilized hydrogels were utilized to induce hypoxia for *in vitro* cell culture. Anchorage-independent acute myeloid leukemia cells (Molm14) and adherent hepatocarcinoma cells (Huh7) were used to evaluate the effect of enzyme induced hypoxia on cancer cell fate, including cell viability, proliferation, and hypoxia-associated gene expression. Finally, immobilized GOX hydrogels were used to induce hypoxia within specialized channel slides for future investigation on the effect of oxygen gradients on cell migration.

2.2 Objective 1: Synthesize enzyme immobilized hydrogels for inducing hypoxia.

This objective focuses on the effect of using GOX and CAT to control O_2 tension in solution and in hydrogel. GOX was modified with Acryl-PEG-SVA to yield GOX_{PEGA}, which permitted its covalent immobilization within PEGDA hydrogels. O_2 tension was characterized both at the interior and exterior of the GOX_{PEGA} hydrogels. The effects GOX_{PEGA} gels combined with CAT and additional glucose on O_2 tension and H_2O_2 production were also examined.

2.3   Objective 2: Evaluate hypoxia inducible hydrogels on cancer cell fate *in vitro.*

This objective focuses on developing the GOX_{PEGA} gel system for *in vitro* hypoxic cell culture. The cytocompatibility of enzyme-free and GOX_{PEGA}-immobilized PEGDA hydrogels was evaluated using anchorage-dependent HCC line Huh7 and anchorage-independent AML line Molm14. The expression of hypoxia associated genes, including CA9 and LOX, were examined to assess the ability of the GOX_{PEGA} hydrogels to induce hypoxic cellular response.

2.4   Objective 3: Establish hypoxia gradients using enzyme immobilized hydrogels.

For the third objective, the goal was to develop a gradient of O_2 within a commercially available channel slide suitable for cell culture and *in situ* monitoring of cell migration. GOX_{PEGA} gels were placed within two reservoirs connected by a cell culture channel. O_2 content was evaluated in the reservoirs open to ambient air. The O_2 data obtained from the two reservoirs were used in conjunction with a mathematical model to semi-empirically predict the O_2 concentration along the channel as a function of time.

3. MATERIALS AND METHODS

3.1 Materials

Linear PEG (Mn = 2 kDa) was purchased from Sigma-Aldrich. Glucose oxidase (0243-500KU) and catalase (LS001847) were purchased from Amresco and Worthington Biochemical, respectfully. Acrylate-PEG-succinimidyl valerate (Acryl-PEG-SVA) was obtained from Laysan Bio Inc. Zeba Spin Desalting Columns (7K MWCO), 2,4,6-trinitrobenzene sulfonic acid (TNBSA), and β-D-glucose were purchased from Thermo Scientific. Penicillin-streptomycin, antibiotic-antimycotics, fetal bovine serum (FBS), Roswell Park Memorial Institute media (RPMI), and Dulbeccos modified Eagles medium (DMEM) were acquired from Life Technologies. HEPES and Dulbeccos phosphate-buffered saline (DPBS) were purchased from Lonza. Membrane culture plate inserts (PIXP-012-50) were purchased from EMD Millipore. Tryphan blue and AlamarBlue reagents were purchased from Mediatech and Fisher Scientific, respectfully.

3.2 Macromer synthesis and characterization

PEG-diacrylate (PEGDA) was synthesized according to an established protocol [44] and characterized with 1H-NMR (Bruker 500). The degree of PEGDA functionalization was around 89% (Figure A.1). Photoinitiator lithium aryl phosphonate (LAP) was synthesized as described elsewhere [45].

For covalent enzyme immobilization within the hydrogel, glucose oxidase was acrylated using Acryl-PEG-SVA [27, 46]. Briefly, the enzyme was first dissolved at 20 mg/mL in PBS supplemented with 2 mM EDTA (pH 8.5) and 50 mM sodium carbonate. Acryl-PEG-SVA was added at 200x molar excess to enzyme concentration and the reaction was allowed to proceed at room temperature for 2 hours with stir-

ring. During the reaction, primary amines on the surface of the enzyme reacted with SVA groups to afford PEG-acrylate (PEGA)-modified GOX (GOX_{PEGA}). Unreacted macromers were removed using size exclusion chromatography columns (Zeba Spin Desalting column). Un-modified GOX at the same concentration was also passed through the columns and used as controls to account for any loss/entrapment of enzyme within the columns. Following synthesis, both GOX and GOX_{PEGA} were assayed using TNBSA assay to determine the degree of PEGA functionalization. For each assay, enzyme samples were diluted to 30-35 μg/mL. A series of lysine hydrochloride solutions (0-10 μg/mL, 200 μL/well) were used as standards. 100 μL of 0.01% TNBSA reagent was added into wells of a 96-well plate, which was sealed and incubated at 37°C for 2 hours, followed by cooling for 5 minutes. Absorbance at 335 nm was measured using a microplate reader (SynergyHT BioTek). The degree of PEGA functionalization on GOX was determined as the concentration of remaining amine groups on GOX_{PEGA} over that of the un-modified GOX.

3.3 Characterization of enzymatic activity of GOX_{PEGA}

To examine the enzyme activity of GOX_{PEGA}, O_2 consumption in the presence of the enzyme and glucose was quantified. The changes in substrate (i.e., O_2) content over time in the presence of GOX or GOX_{PEGA} ($V_o = \Delta[O_2]$ / ΔTime) was defined as the reaction velocity. Enzyme was dissolved PBS (pH 7.4) at 0.13 μM in a 2 mL microtube with constant stirring at 25°C. The O_2 consumption reactions were carried out under ambient air with constant O_2 diffusion from the air to mimic actual cell culture conditions. The Stock β-D-glucose solution was injected at the start of every measurement to give starting concentrations of 0.30 to 25 mM $[S]_i$. Dissolved O_2 concentration was monitored for 3 minutes using an O_2 probe and meter (Microx4, PreSens). O_2 contents were plotted as a function of time and the initial linear portion of the curve was used for V_o calculation (change in substrate concentration over time). Non-linear regression analysis and curve fitting was applied to paired V_o and $[S]_i$ using the equation $V_o = V_{max}[S]/(K_m + [S])$. In the equation, V_{max} is the theoretical

maximum enzyme reaction velocity and K_m is the Michaelis-Menten constant, which is the substrate concentration at which half of V_{max} is reached.

3.4   Synthesis and characterization of enzyme-immobilized hydrogels

All macromer solutions were sterilized by passing through 0.22 μm syringe filters. PEGDA hydrogels (15 wt%) were polymerized aseptically through radical mediated photopolymerization in the absence or presence of GOX_{PEGA} monomer (6 mg/mL), and LAP (1 mM) as the photoinitiator. 60 μL gels were injected between two glass slides separating by Teflon spacers (2 mm) and gelation was initiated with a UV lamp (365 nm, 5 mW/cm^2, 2 min exposure). Following photopolymerization, hydrogels ($\sim$3.1 mm diameter x 2 mm thickness) were incubated in DPBS for 24 hours at 37°C.

O_2 concentration in solution was measured with a dipping-type O_2 sensor (Microx4, PreSens). For solution based measurements, the probe was extended to $\sim$2 mm above the bottom of the 24 well plate or 1 mm above the gel ($\sim$2 mm from the liquid-air interface). To measure the H_2O_2 produced during the reactions, 10 μL aliquots of the solutions were collected and quantified with a Quantichrom Peroxide Assay Kit following the manufacturers protocol (BioAssay Systems).

3.5   Cell culture and viability assays

A suspension cell type, human acute myeloid leukemia (AML) cells Molm14, was purchased from Leibniz Institute, German Collection of Microorganisms and Cell Cultures. Cells were maintained in RPMI media supplemented with 10% fetal bovine serum (FBS) and 1% penicillin-streptomycin, 25 mM HEPES, and 25 mM β-D-Glucose. 400,000 cells/mL of Molm14 cells were seeded per well in non-treated 24 well plates. GOX_{PEGA} gels (15 wt% PEGDA, 6 mg/mL GOX_{PEGA}, 60 μL per gel) were added to half of the wells (one gel per well) containing 0.54 mg/mL CAT. Remaining wells were placed with gels without immobilized enzyme. *In vitro* O_2 concentration was measured $\sim$1 mm above the hydrogel with a dipping-type O_2 sensor (PreSens). Adherent cell type human hepatocarcinoma cells (Huh7) were grown in

high glucose DMEM supplemented with 10% FBS, 1% antibiotic antimycotics, and 25 mM HEPES. Cells were seeded on treated 24 well plates with 1 mL per well of cell suspension (60,000 cells/mL) and allowed to grow/spread for 48 hours prior to the onset of the experiments, at which time (labeled as 0 hours) culture media was refreshed in all wells. At the onset of the experiment, membrane inserts containing GOX_{PEGA} gels were placed in the wells and the media was supplemented with 0.54 mg/mL CAT. Half of the wells only had media refreshed and were used as control groups for the experiment (no enzyme added).

Molm14 cell viability and density were characterized by tryphan blue staining and counting with a hemocytometer. AlamarBlue reagent (10x dilution in media) was used for assaying metabolic activity of Huh7 cells. After a 90 minute incubation period, 200 μL from each well was transferred to a clear 96-well microplate and read for fluorescence (excitation/emission: 560/590 nm).

3.6   RNA isolation and real time PCR

RNA isolation was carried out using NucleoSpin RNA II kit (Clontech). Briefly, 600 μL of lysis buffer was added to each well containing cells. Cell lysates were snap frozen and stored in -80°C until assay. After thawing the lysates, 600 μL of 70% RNase free ethanol was added, pipetted vigorously, and then run through NucleoSpin RNA columns. After desalting/purification steps, RNA was eluted with DNase/RNase-free H2O and quantified by spectroscopy (NanoDrop 2000, Thermo Scientific). Isolated RNA was stored at -80°C.

Complementary DNA was generated from the isolated total RNA by using Prime-Script RT reagent kit (Clontech, TaKaRa). Gene expression was analyzed by real time quantitative PCR using SYBR Premix Ex Taq II Kit (Clontech, TaKaRa). The kit components, cDNA, and primers were mixed in a PCR plate and analyzed on a 7500 Fast Real-Time PCR machine (Applied Biosystems). Thermocycling parameters were one cycle at 95°C for 30s, followed by 95°C for 3s, 60°C for 30s, and repeat for 45 cycles. Gene expression results were analyzed using $2^{-\Delta\Delta CT}$ methodology. For each

experimental condition, cycle count was first standardized to ribosomal 18S house-keeping gene (ΔCT level) and then normalized with respect to the media control group for that specific time point ($\Delta\Delta$CT level; media control values were set as one-fold). Table A.1 lists all primer sequences used for real-time PCR.

3.7   Oxygen Gradient Development & Mathematical Modeling

For O$_2$ gradient experiments, specialized channel slides were purchase from ibidi (GmbH, Munich, Germany, CAT# 80111, μ-Slide-1). Each slide had two reservoirs (A and B) connected by a 50 mm long channel (Figure 3.1):
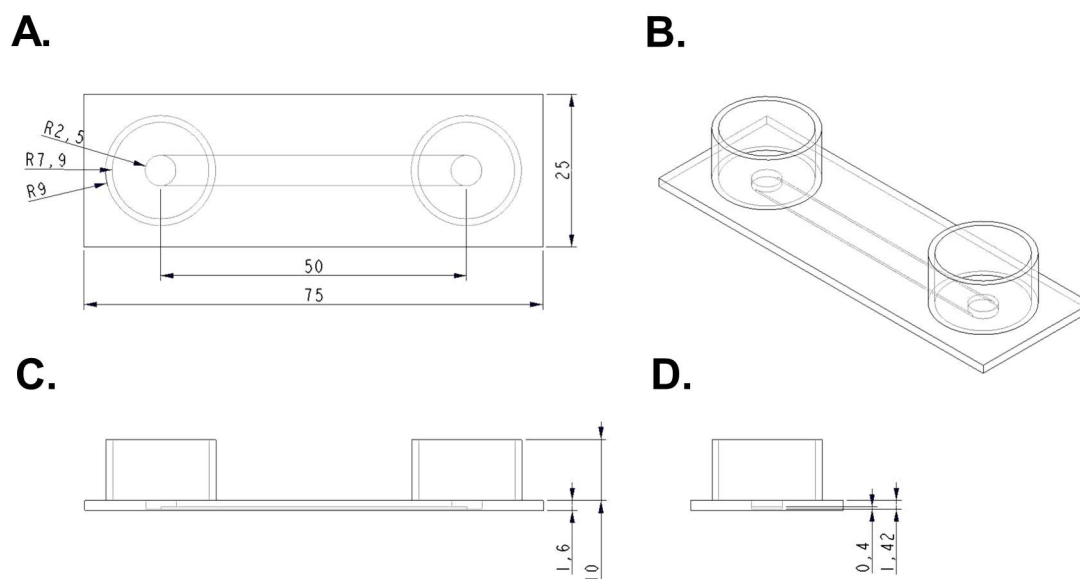
Fig. 3.1. CAD diagram of the ibidi channel slide with approximate dimensions. (A) Top view. (B) Isometric view. (C) Front view. (D) Side view. According to manufacturer specifications, channel volume is 100 μL and reservoir volume is 600 μL (each). Diagrams were made using PTC Creo Parametric.

Plates were filled with 25 mM β-D-glucose solution supplemented with 1% antibiotic antimycotics, and one GOX$_{PEGA}$ gel was placed in each well (Figure 3.2). O$_2$ concentrations as a function of time were recorded at $\sim$1 mm above the hydrogel with

a needle-type O_2 sensor (PreSens). All reactions were carried out within a humidified incubator at 37°C.
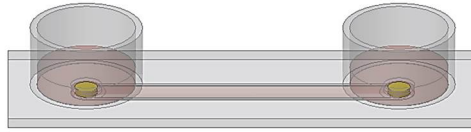
Fig. 3.2. Diagram of an ibidi channel slide containing GOX_{PEGA} hydrogels (yellow) and DPBS (red). Diagrams were made using PTC Creo Parametric.

With the given experimental setup, O_2 concentration could not be measured directly within the channel. Therefore, Ficks Law of diffusion in one-dimension was chosen to predict the concentration of O_2 (C) as a function of time (t) and distance (x) across the channel (Equation 3.1):

$$\frac{\partial C}{\partial t} = D \frac{\partial^2 C}{\partial x^2} \tag{3.1}$$

Here, D is the diffusivity of O_2 in solvent, C is the concentration of O_2 in the channel, t represents time, and x is the length of the channel. Considering the non-steady state nature of O_2 concentration over time in the ibidi channel system, numerical methods were used to empirically approximate O_2 concentration in the channel [47]. Specifically, a centered finite-divided difference formula for the space derivative (Equation 3.2) and a finite-divided difference formula for the time derivative (Equation 3.3) were used to approximate the non-steady state diffusion. Substitution of Equations 3.2 and 3.3 into Equation 3.1 yields the numerical approximation of Ficks 1D-diffuison in Equation 3.4:

$$\frac{\partial^2 C}{\partial x^2} \approx \frac{C_{I+1}^L - 2C_I^L + C_{I-1}^L}{\Delta x^2} \tag{3.2}$$

$$\frac{\partial C}{\partial t} \approx \frac{C_I^{L+1} + C_I^L}{\Delta t} \tag{3.3}$$

$$\frac{C_I^{L+1} + C_I^L}{\Delta t} = D \frac{C_{I+1}^L - 2C_I^L + C_{I-1}^L}{\Delta x^2} \tag{3.4}$$

Superscript and subscript within the numerical approximations denote data node locations of time (I) and space (L). Equation 3.4 can be algebraically rearranged to solve for the next unknown time increment:

$$C_I^{L+1} = C_I^L + \lambda(C_{I+1}^L - 2C_I^L + C_{I-1}^L), \quad \lambda = \frac{D\Delta t}{(\Delta x)^2} \qquad (3.5)$$

Equation 3.5 is applicable to all distances between two points and provides an empirical means to calculate values as a function of time and distance for future points in the channel (Figure 3.3).
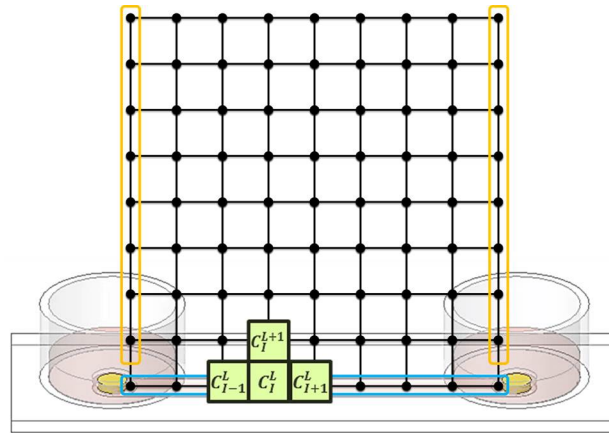
Fig. 3.3. Numerical method for simulating oxygen tension within an ibidi channel slide. Initial condition nodes are outlined in blue. Boundary condition nodes are outlined in yellow. The stacked green boxes represent the node values used for averaging for a given set of time and location O_2 concentrations as describe by Equation 3.5.

Initial conditions within the channel were set to normoxic O_2 concentration ($\sim19\%$) and boundary O_2 concentrations at x = 0 mm and x = 50 mm were set to values measured experimentally in reservoirs A and B. Diffusivity used for O_2 in the aqueous environment was $2.7\mathrm{x}10^{-5}$ cm^2/s. Step values were 0.25 hour for time and 5 mm for distance. O_2 values for every replicate in every experimental condition had numerical mesh data calculated and then averages were calculated for corresponding time and distance nodes among the replicates.

3.8   Statistics

GraphPad Prism 5 was used for all curve fitting and statistical analyses. Significance comparison between experimental groups was performed using Two-Way ANOVA with Bonferroni post testing. Michaelis-Menten parameters for GOX and GOX_{PEGA} were generated with the non-linear regression suite in GraphPad Prism 5 software. O_2 gradient mathematical modeling was done in Matlab and the code can be found in the appendix section. All experiments were conducted a minimum of three times with data presentation as the mean $\pm$ standard error of the mean (SEM). One, two, or three asterisks represent $p < 0.05$, 0.01, or 0.001, respectively.

4. RESULTS AND DISCUSSION

4.1 Enzyme-mediated hypoxia generation

GOX/CAT systems have been used to induce pH changes in aqueous environment due to the production of gluconic acid (Figure 1.1). To gain insights into the capability of this enzymatic system on inducing hypoxia in solution, the reduction of O_2 was quantified in aqueous buffers supplemented with different concentrations of GOX in the absence (Figure 4.1A) or presence (Figure 4.1B) or CAT. The O_2 tensions of the buffers were monitored using an O_2 sensor and recorded as a function of time. As expected, higher concentrations of GOX were able to deplete O_2 faster. As shown in Figure 4.1A, O_2 tension was reduced within 5 minutes to ~6% and ~2.5% when 2.25 μg/mL or 4.5 μg/mL of GOX was added, respectively. With the inclusion of 9.8 μg/mL of CAT in the solution, the rate of O_2 consumption was slowed down to ~9% and 3.2% within 5 minutes (Figure 4.1B). The decrease in O_2 consumption is not surprising as the addition of CAT produces one-half mole of O_2 per mole of H_2O_2 consumed.
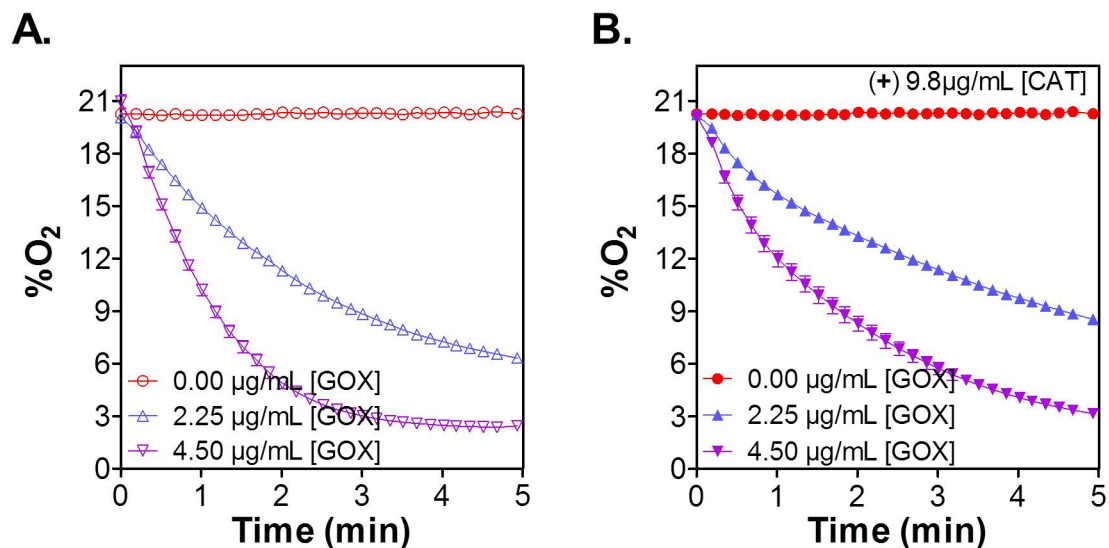
Fig. 4.1. Enzymatic generation of aqueous oxygen tension. (A) O_2 consumption profile for GOX. (B) O_2 consumption profile for GOX in the presence of 9.8 μg/mL CAT. All reactions were carried out in PBS, pH 7.4 at room temperature with 25 mM β-D-Glucose. (Mean $\pm$ SEM, n $\geq$ 3).

In order to fabricate enzyme-immobilized hydrogels capable of inducing hypoxia, the primary amine groups on GOX were functionalized with Acryl-PEG-SVA (Figure 4.2) [27, 46]:
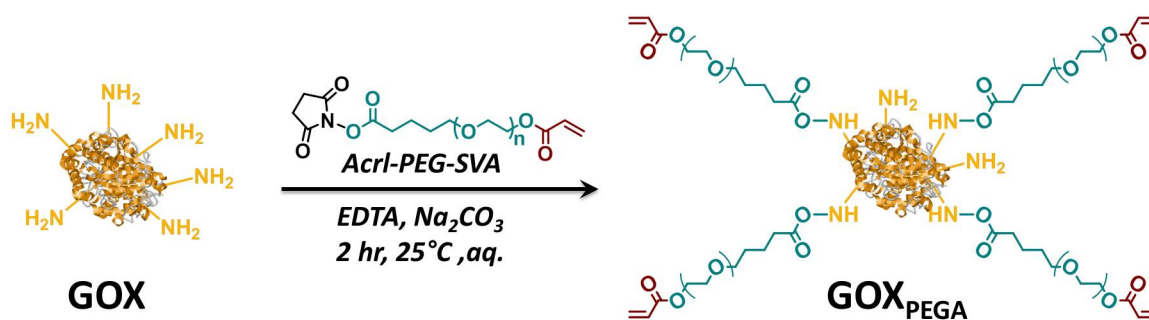
Fig. 4.2. Reaction scheme of GOX modification using Acryloyl-PEG-SVA. Protein structure for GOX was obtained from RCSB PDB (3QVP).

TNBSA assay results showed an average of $93 \pm 1.7\%$ (Mean $\pm$ SEM, N = 5) of the primary amines on the surface of the enzyme were functionalized with Acryl-PEG. The acrylate moieties on the surface of Acryl-PEG-GOX (i.e., GOX_{PEGA}) permit its homopolymerization with PEGDA to afford enzyme-immobilized hydrogels.

The modification, however, could affect the ability of GOX_{PEGA} to consume O_2. As shown in Figure 4.3A, while un-modified GOX caused rapid O_2 reduction (from $\sim 20\%$ to $\sim 3.2\%$ in 5 minutes) in solution, the ability of GOX_{PEGA} to consume O_2 was hindered after Acryl-PEG-SVA modification (from $\sim 20\%$ to $\sim 5.9\%$ within 5 minutes). To quantify the impact of polymer modification on its enzyme activity, reaction velocities of GOX and GOX_{PEGA} were measured and compared in Figure 4.3B.
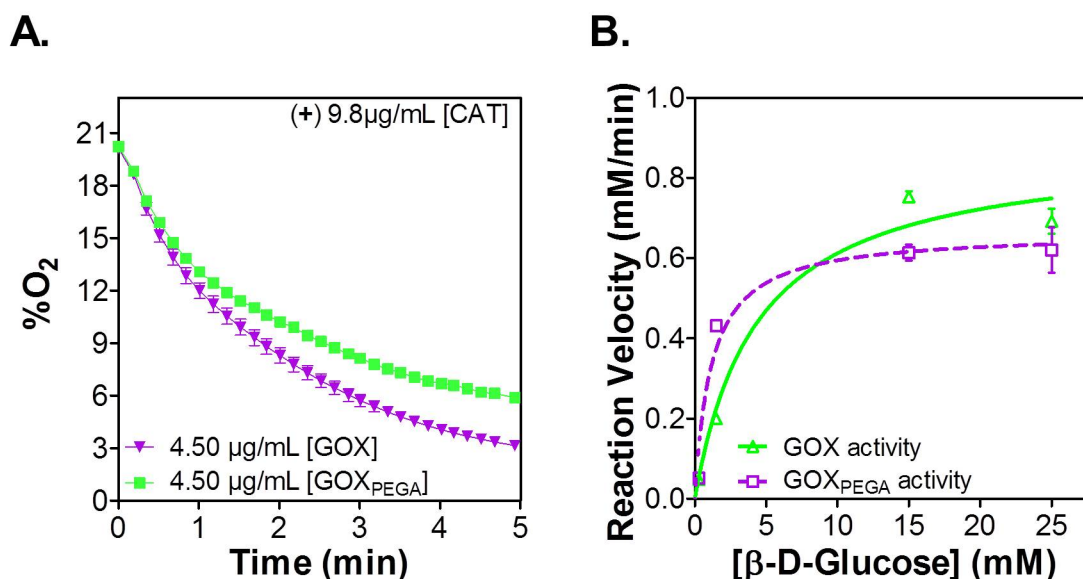
Fig. 4.3. Effect of GOX modification on oxygen consumption profiles. (A) O_2 consumption profile using soluble GOX or GOX_{PEGA}, 9.8 μg/mL CAT, and 25mM β-D-Glucose. (B) Reaction velocity of O_2 consumption by GOX or GOX_{PEGA} as a function of substrate β-D-glucose concentration. Values were generated from using 0.260 μM GOX or GOX_{PEGA} with 0.30 to 25 mM of β-D-glucose. All reactions were carried out in pH 7.4 pBS with constant stirring at 25°C. (Mean $\pm$ SEM, n $\geq$ 3).

Michaelis-Menten enzyme kinetic parameters were listed in Table 4.1. Maximum reaction velocity, V_{max}, was reduced for GOX_{PEGA} to 0.664 mM·min^{-1}, or approximately 75% of that for GOX (0.880 mM·min^{-1}). Additionally, K_m, an estimate of the dissociation constant for enzyme and substrate, was also decreased for GOX_{PEGA} at 1.1173 mM versus GOX at 4.380 mM.

Table 4.1. Michaelis-Menten constants of GOX and GOX_{PEGA}.

	V_{max} (mM·min^{-1})	K_m (mM)
GOX	0.88 ± 0.05	4.38 ± 0.90
GOX_{PEGA}	0.66 ± 0.03	1.17 ± 0.28

To evaluate the ability of the enzyme system to maintain hypoxia, O_2 content measurements were carried out for 72 hours. Figure 4.4 shows long term solution hypoxia induced by GOX or GOX_{PEGA} in the absence (Figure 4.4A) and presence (Figure 4.4B) of CAT. Between GOX and GOX_{PEGA} groups, O_2 content was very similar for all time points. Within the first 24 hours, O_2 was maintained below 5% but gradually increased to ~13% by 72 hours (Figure 4.4A). The addition of CAT did not affect O_2 content, which was below 5% in the first 24 hours for both GOX and GOX_{PEGA}. The O_2 content in both conditions rose to ~16% and ~18% at 50 and 72 hours, respectively.
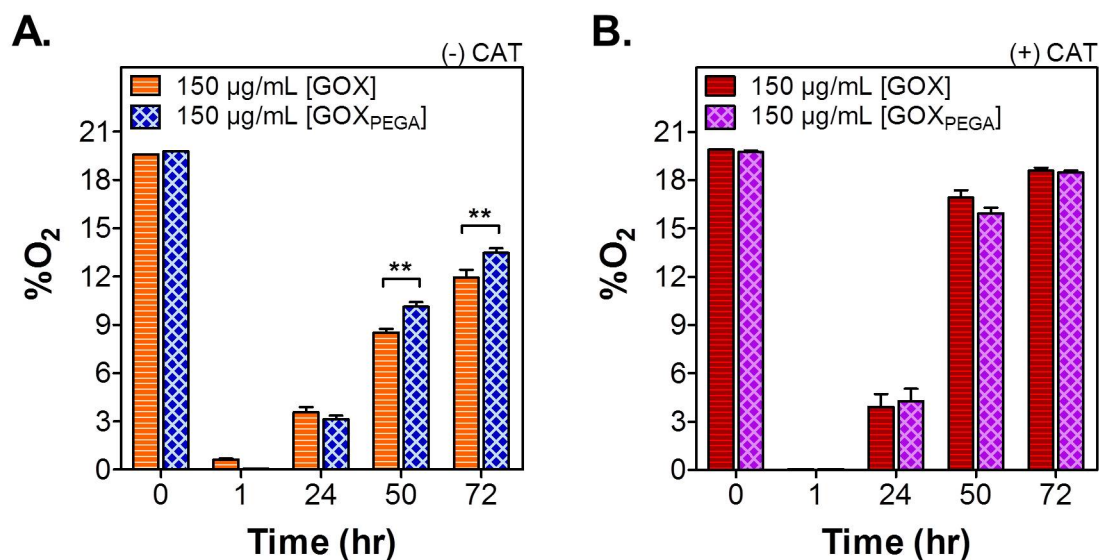
Fig. 4.4. Effect of GOX modification on oxygen consumption profiles over extended time periods. (A,B) O_2 consumption profiles of unmodified and acrylated GOX in the absence (B) or presence (A) of soluble CAT (450 μg/mL). All reactions were carried out in pH 7.4 PBS, at 25°C, with 25 mM β-D-Glucose. (**p < 0.01. Mean ± SEM, n ≥ 3).

4.2 GOX$_{PEGA}$-immobilized hydrogels for inducing hypoxia

GOX$_{PEGA}$ was covalently immobilized within PEGDA hydrogels to provide a simple method for inducing solution hypoxia (Figure 4.5) [46]:
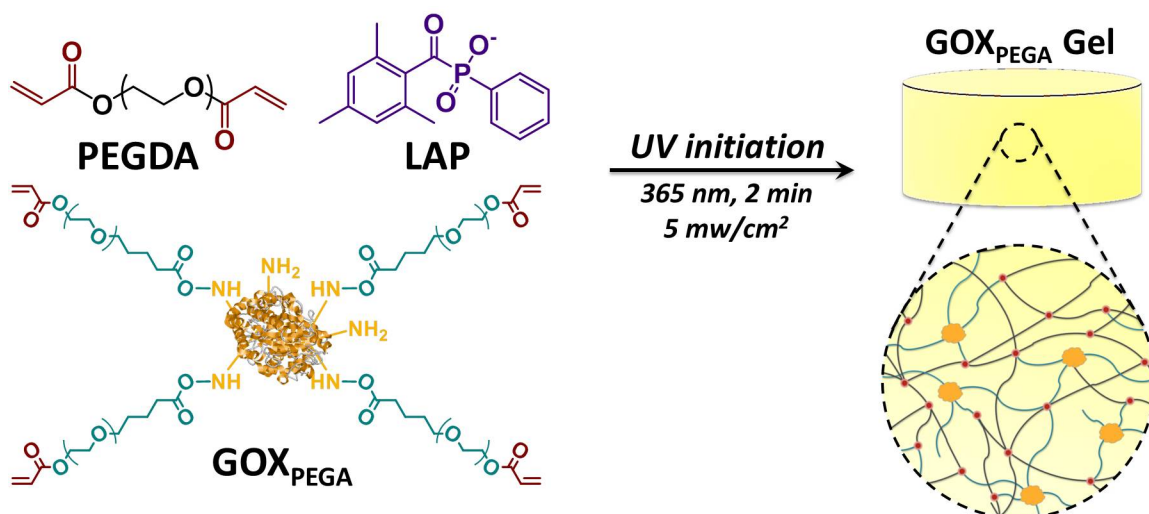
Fig. 4.5. Schematic of enzyme-immobilized hydrogel formation from poly(ethylene glycol)-diacrylate (PEGDA), lithium arylphosphinate (LAP) and PEG-acrylate modified glucose oxidase (GOX_{PEGA}).

The ability of the immobilized enzyme to reduce O_2 in the surrounding solution and within the gel was measured with a needle type optical probe as shown in Figure 4.6.
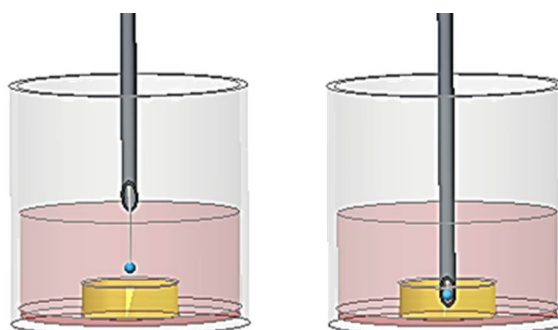
Fig. 4.6. Schematic of O_2 measurement within and outside of PEGDA hydrogel. The sensor probe was fully extended from the needle for measuring O_2 tension exterior to the hydrogel (left). To measure O_2 content at the interior of the hydrogel (right), the optic fiber was recessed within its needle housing to prevent damage of the gel matrix to the probe. After penetration the fiber was extended to the tip of the needle cannula so that it was exposed to the interior of the hydrogel.

With the needle type O_2 probe, it was possible to measure O_2 content outside (left panel) or inside (right panel) the GOX_{PEGA} immobilized hydrogels (Figure 4.7B). Control experiments using hydrogels without enzyme immobilization (i.e., (-) GOX_{PEGA}) showed that O_2 content remained close to normoxia (17-20% O_2 , Figure 4.7A). Furthermore, there was no significant difference between O_2 content within or outside of the enzyme-free hydrogels. With the use of GOX_{PEGA} immobilized PEG hydrogels, however, there was a rapid drop in the exterior (i.e., outside of the GOX_{PEGA} immobilized hydrogel) O_2 tension within one hour, a level similar to that with soluble enzyme (Figure 4.4A). O_2 tension was roughly at $\sim$8% O_2 for 48 hours in solution with the GOX_{PEGA} hydrogels. Conversely the O_2 tension within the GOX_{PEGA} hydrogel quickly reached and maintained near anoxia ($\sim$0% O_2) for 48 hours. The O_2 tension at the gel exterior had increased to $\sim$15% by 120 hours, while that in the gel interior was still below 2%.
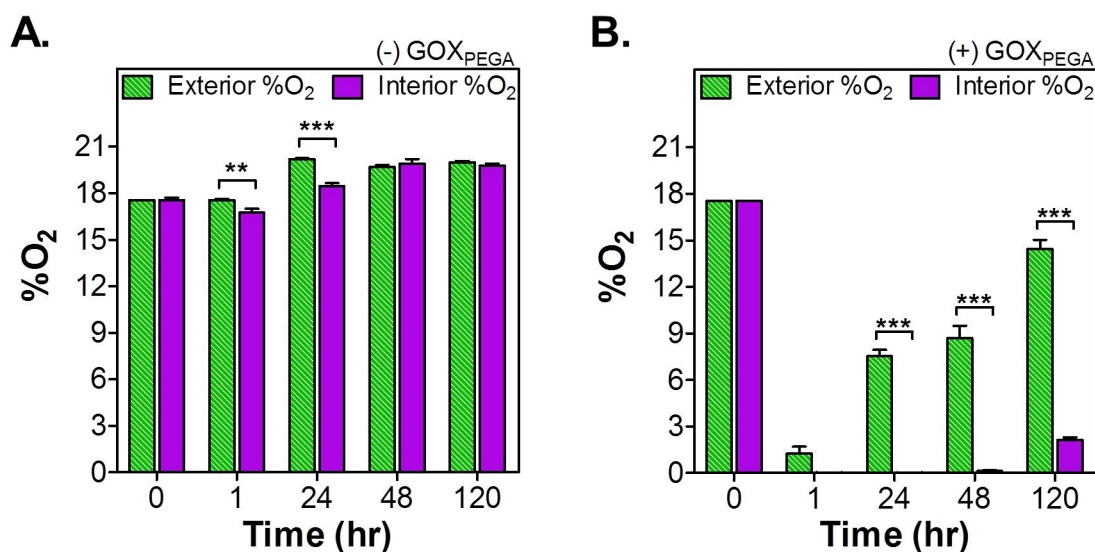
Fig. 4.7. Interior and exterior O_2 consumption for immobilized GOX_{PEGA} hydrogels. Hydrogel (120 μL, with or without 4 mg/mL GOX_{PEGA}) was formed by 8 wt% PEGDA using 1 mM LAP as the photoinitiator. (**p < 0.01, ***p < 0.001. Mean $\pm$ SEM, n $\geq$ 3).

4.3 Combined GOX$_{PEGA}$-immobilized hydrogels and soluble CAT for inducing hypoxia

Next, GOX$_{PEGA}$-immobilized hydrogels were placed in buffer solution containing catalase and the solution O$_2$ content was measured (Figure 4.8A). After placing the GOX$_{PEGA}$ gel, hypoxia was induced and sustained for at least 6 hours. By 24 hours, the O$_2$ content in solution without CAT returned to ∼14%, whereas it remained ∼6% in the presence of CAT. By 48 hours, the O$_2$ content returned to ∼14% and ∼16% for solution with or without CAT, respectively. Increasing percent O$_2$ over time would indicate that some degree of enzyme activity was lost. Figure 4.8B shows that, in the presence of CAT, H$_2$O$_2$ concentrations were 2 mM and 5 mM at 24 and 48 hours, respectively. In the absence of CAT, however, H$_2$O$_2$ concentration increased to ∼9 mM at both time points.
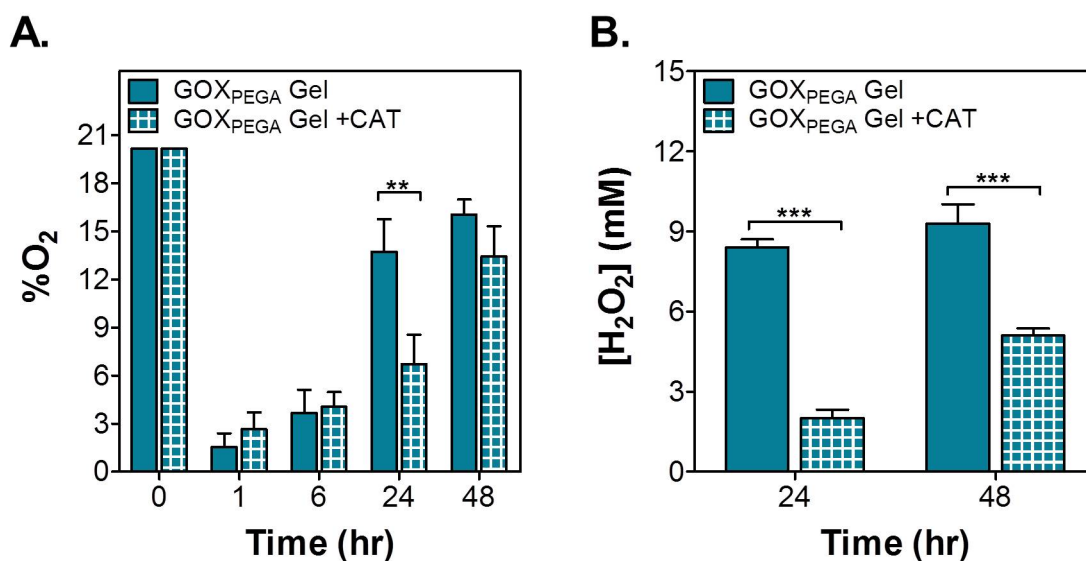
Fig. 4.8. Effect of soluble CAT addition on O$_2$ consumption and H$_2$O$_2$ production by GOX$_{PEGA}$ gels. (A) O$_2$ tension. (B) H$_2$O$_2$ accumulation. Hydrogels (60 μL) were formed by 15 wt% PEGDA co-polymerized with 6 mg/mL GOX$_{PEGA}$. CAT group was 0.54 mg/mL in solution. All reactions were carried out in pH 7.4 DPBS at 37°C. (**p < 0.01. ***p < 0.001. Mean ± SEM, n ≥ 3).

To ensure that glucose was not exhausted during the GOX reaction, the solution was supplemented with additional β-D-glucose at later time points. A 50 μL shot of β-D-glucose (at 50 mM) was added to the solution (1000 μL) containing GOX_{PEGA} gel 5 minutes before O_2 detection (at 24 and 48 hours). As shown in Figure 4.9A and 4.9B, bolus addition of glucose did not significantly affect the O_2 content or the H_2O_2 concentration in solution.
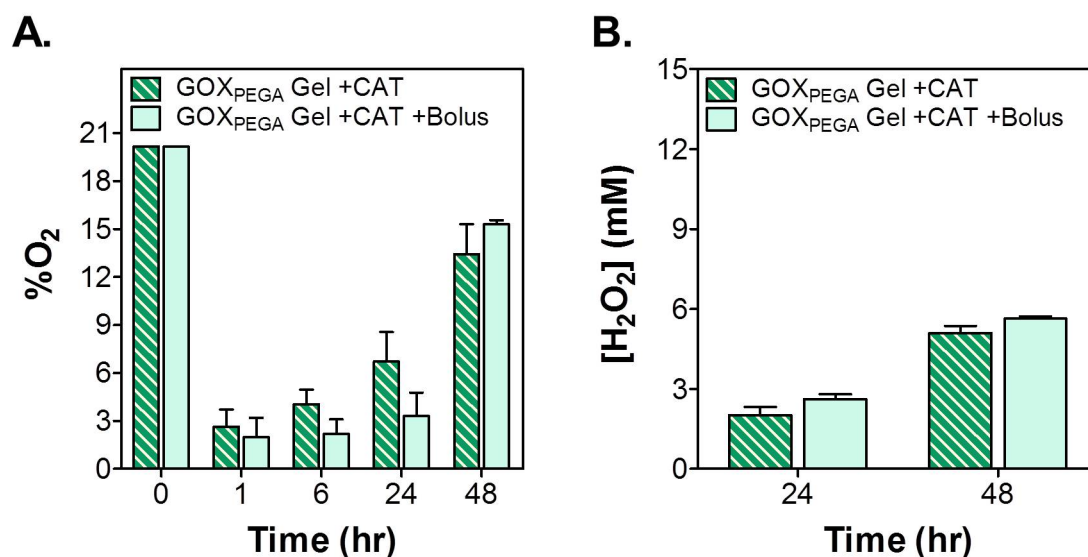
Fig. 4.9. Effect of additional glucose and soluble CAT addition on O_2 consumption and H_2O_2 production by GOX_{PEGA} gels. (A) O_2 tension. (B) H_2O_2 accumulation. Additional bolus injections of glucose (50 μL of 500 mM) were delivered 5 minutes before measuring O_2 at 24 and 48 hour time points. Hydrogels (60 μL) were formed by 15 wt% PEGDA co-polymerized with 6 mg/mL GOX_{PEGA}. All reactions were carried out in pH 7.4 DPBS at 37°C with 0.54 mg/mL CAT in solution. (Mean $\pm$ SEM, n $\geq$ 3).

To test whether replacing a new GOX_{PEGA} gel would prolong hypoxia in the solution, the old gel was removed after 24 hours and a freshly prepared GOX_{PEGA} gel (identical formulation) was placed in the same well. Additionally, freshly prepared CAT solution was also added. Figure 4.10 shows that the O_2 content was maintained at ~5% at 30 hours (i.e., 6 hours post gel replacement), whereas the O_2 content was

~9% in the control group (i.e., without replacing GOX_{PEGA} gels). However, the O_2 content in both conditions increased to above 14% at 48 hours.
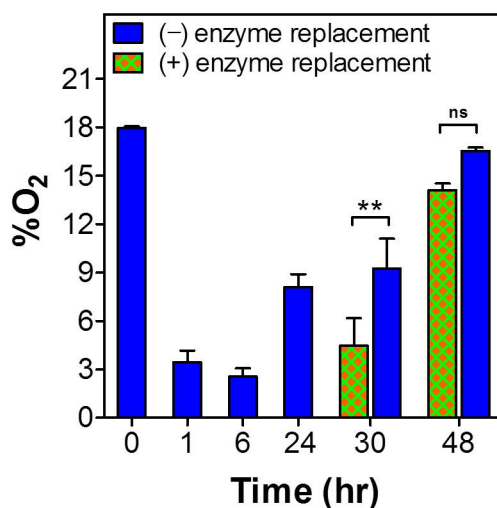
Fig. 4.10. Effect of replacing GOX-immobilized hydrogel on solution O_2 tension. Old GOX-immobilized gels were replaced with new GOX-immobilized gels along with fresh CAT after 24 hours. Hydrogels (60 μL) were formed by 15 wt% PEGDA copolymerized with 6 mg/mL GOX_{PEGA}. All reactions were carried out in pH 7.4 DPBS at 37°C with 0.54 mg/mL CAT in solution. (**p < 0.01. Mean $\pm$ SEM, n $\geq$ 6).

4.4 Cytocompatibility of enzyme-immobilized hydrogels

Figure 4.11 shows the cytocompatibility of enzyme-free (i.e., PEGDA only) and GOX-immobilized hydrogels. Molm14 cell viability was maintained above 95% over the course of 48 hours in the presence of an enzyme-free PEGDA hydrogel (Figure 4.11A). These cells were also proliferating over time, as indicated by steady increase in cell density (Figure 4.11B). When a GOX_{PEGA} gel was placed together with Molm14 cells (with media-supplemented CAT), cell viability in the initial 24 hours was comparable to that in the media-only control (around 90%, Figure 4.11C). However, after 48 hours of *in vitro* culture, Molm14 cell viability declined sharply to ~55%. In

addition to the decreased cell viability after 48 hours, a similar trend can be seen with cell density over time (Figure 4.11D). Specifically, there was no significant difference in cell density between the control and experimental group at 6 hours (i.e., $\sim 3.6 \times 10^5$ cells/mL). By 48 hours the Molm14 cell density in the media-only control group had increased to $\sim 5.5 \times 10^5$ cells/mL, whereas the Molm14 cell density in the GOX-immobilized hydrogel group decreased significantly to $\sim 2.2 \times 10^5$ cells/mL.
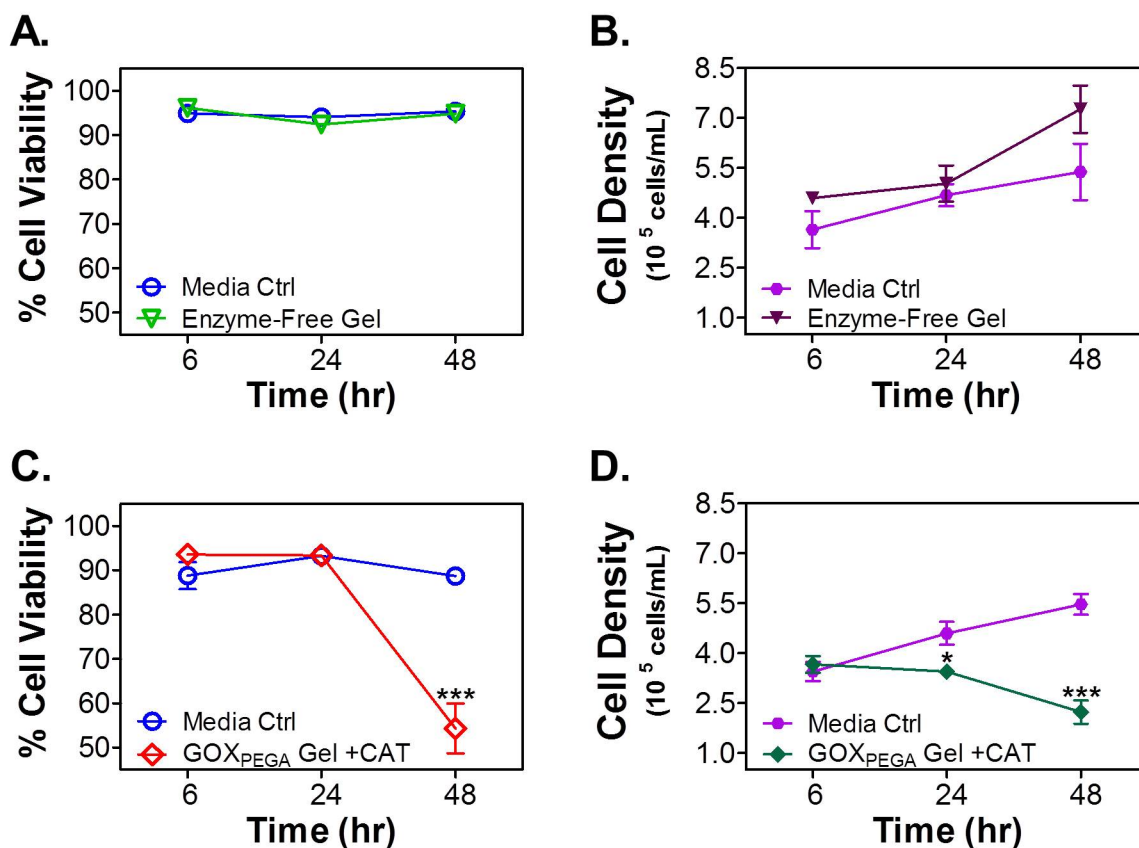
Fig. 4.11. Cytocompatibility of PEGDA hydrogels with or without immobilized GOX_{PEGA}. Molm14 cell viability (A, C) and density (B, D) when cultured in the absence (Enzyme-free Gel; A & B) or presence (C, D) of immobilized (6 mg/mL) GOX_{PEGA} Gel + CAT. Hydrogels (60 μL) were formed by 15 wt% PEGDA copolymerized with 6 mg/mL GOX_{PEGA}. CAT in media was 0.54 mg/mL. (*p < 0.05. ***p < 0.001. Mean $\pm$ SEM, n $\geq$ 3).

4.5 Enzyme-induced hypoxia in the presence of cells

The main focus of this study was to develop an enabling material technology for facilitating a wide variety of *in vitro* cancer cell culture. Anchorage-independent acute myeloid leukemia (AML) cell line Molm14 and anchorage-dependent hepatocarcinoma cell (HCC) line Huh7 were chosen to test the utility of the hypoxia-inducing hydrogels [46]. The survival and progression of these cells, just like many other cancer cell types, were significantly affected by O_2 tension. GOX_{PEGA} immobilized hydrogels were prepared and added to anchorage-independent Molm14 cells and cultured directly. As shown in Figure 4.12A, solution hypoxia was rapidly induced and maintained below 5% O_2 from 6 to 24 hours. By 48 hours, however, O_2 concentration had risen to near normoxia (17-20% O_2), a result consistent with the cell-free measurements shown in Figure 4.8A and 4.9A.
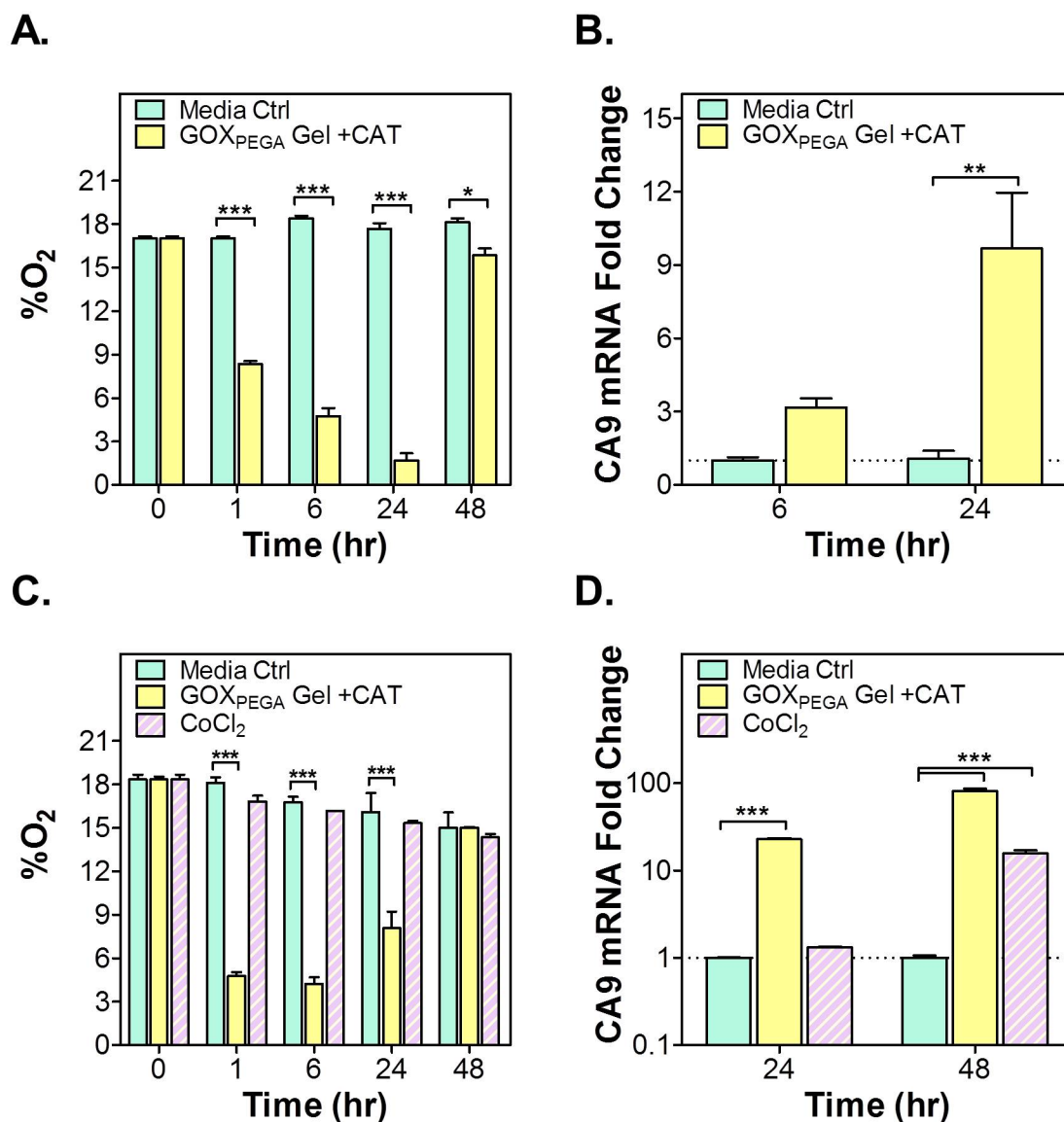
Fig. 4.12. Effect of enzyme-induced hypoxia on cell fate *in vitro*. O$_2$ profile (A, C) and CA9 mRNA expression (B, D) in Molm14 (A, B) or Huh7 cells (C, D) cultured in the presence of a GOX$_{PEGA}$ (6 mg/mL) immobilized 15 wt% PEGDA hydrogel. CAT in media: 0.54 mg/mL. CoCl2 (150 μM) was added separately as an additional control group (*p < 0.05, **p < 0.01, ***p < 0.001. Mean $\pm$ SEM, n $\geq$ 3).

For anchorage-dependent Huh7, GOX$_{PEGA}$ immobilized hydrogels were placed in a standard transwell device and cultured with the cells adhered to the surface of a 24 well plate. The purpose of using a transwell device was to prevent direct contact of

the hydrogel with the cells, which could mechanically disrupt cell attachment. Figure 4.12C shows that O_2 profile development was similar to that for Molm14 cells. Low O_2 concentration was reached quickly and maintained up to 24 hours. By 48 hours, the O_2 content had returned to almost normoxia. As expected, the addition of $CoCl_2$ in cell culture media did not change O_2 tension (Figure 4.12C).

4.6   Effect of enzyme-induced hypoxia on hypoxic gene expression

In addition to cell viability, the expression of hypoxia associated gene carbonic anhydrase 9 (CA9) in Molm14 cells was evaluated at 6 and 24 hours of culture in the presence of GOX-immobilized hydrogel. As shown in Figure 4.12B, the enzyme-induced hypoxia increased the expression of CA9 significantly compared with control groups ($\sim$3-fold and $\sim$10-fold higher at 6 and 24 hours of culture, respectively). For Huh7 cells, the expression of CA9 and lysyl oxidase (LOX) was characterized after the cells were exposed to the enzyme-immobilized hydrogel (Note: no detectable LOX expression was found in Molm14 cells). In selected groups, $CoCl_2$ was added as another control for chemically stabilized hypoxic response. As shown in Figure 4.12D, $CoCl_2$ failed to upregulate CA9 expression in the first 24 hours. After the same period of time in culture, the use of GOX_{PEGA} gels + CAT led to a $\sim$20-fold increase in CA9 expression in Huh7 cells. After 48 hours, the addition of $CoCl_2$ caused $\sim$15-fold upregulation in CA9 mRNA expression, which was much lower than that induced by the enzyme-immobilized hydrogel group ($\sim$80-fold higher). In Huh7 cells, LOX mRNA expression was upregulated only in cells cultured with a GOX_{PEGA} gel ($\sim$2.5 fold, Figure 4.13). The addition of $CoCl_2$ did not increase the expression of LOX in Huh7 cells.
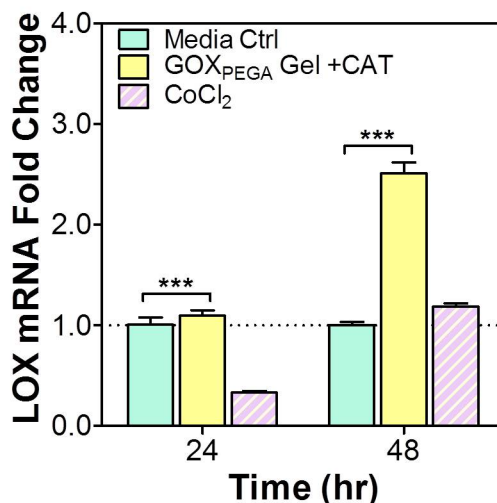
Fig. 4.13. Effect of GOX-immobilized hydrogel on LOX expression in Huh7 cells. $CoCl_2$ (150 μM) was added separately as a control group. Cell culture medium was supplemented with 0.54 mg/mL CAT. Hydrogels (60 μL) were formed by 15 wt% PEGDA co-polymerized with 6 mg/mL GOX_{PEGA}. (***p < 0.001. Mean $\pm$ SEM, n $\geq$ 3).

4.7   Oxygen Gradient Development

To generate O_2 gradients suitable for cell studies, a commercially available channel slide (Figure 3.2) was chosen for its design that permits accommodation of GOX_{PEGA} gels and *in vitro* cell culture. First, O_2 diffusion within the channel was simulated numerically with a finite difference approximation of a one-dimensional diffusion equation (3.5). For boundary conditions, O_2 concentration was held constant at each end of the channel (i.e., in the reservoirs) to represent either O_2-sinks or O_2-sources. For initial conditioning within the channel, O_2 concentration was assumed to be normoxic ($\sim$19% O_2) at all locations at 0 hours of the simulation. The results of numerical simulation for specified boundary and initial conditions are shown in Figure 4.14:
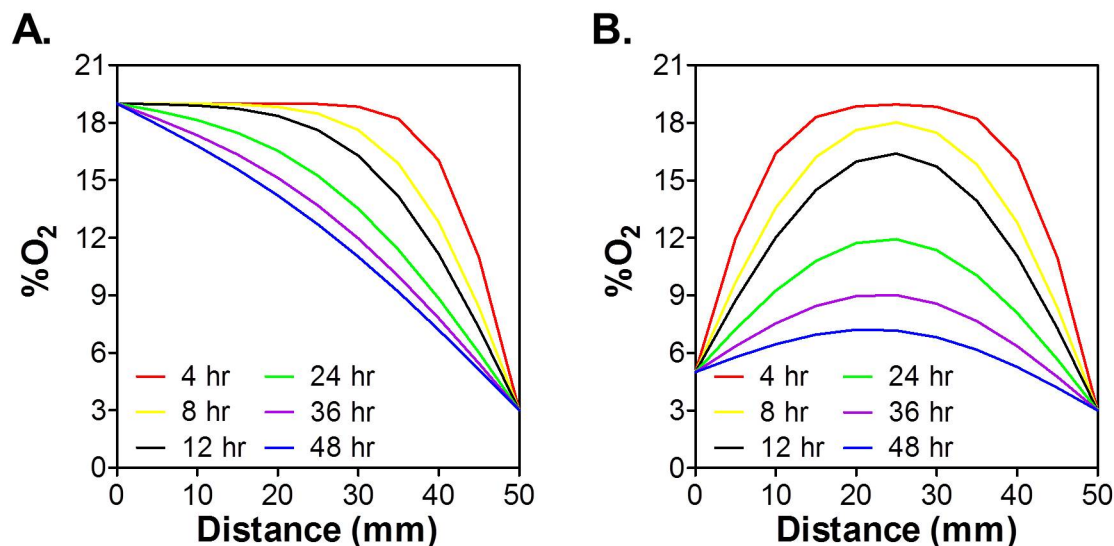
Fig. 4.14. Empirical mesh-modeling of Ficks 1D-diffusion equation for O_2 concentration as a function of time and distance across the channel between the reservoirs. Boundary concentrations at opposite ends of the channel were fixed at (A) 19% and 3% or (B) 5% and 3% O_2.

Figure 4.14A shows the simulation resulting from boundaries at 19% and 3% O_2 at the left and right reservoir, respectively. At 4 hours of simulated O_2 diffusion in the channel, normoxic concentrations of O_2 (17 to 20%) were predicted from the 0-35 mm mark while from the 35-50 mm mark O_2 concentration drops from 18.1% to 3%. At 12 hours, from the 25-50 mm mark, O_2 concentration decreased monotonically from 18.1% to 3%. By 36 hours, O_2 dropped from 17.3% to 3% at the 10-50 mm marks respectively. Finally, at 48 hours, a channel wide gradient from 19% to 3% O_2 was predicted (from 0 to 50 mm mark).

Figure 4.14B shows the numerical simulation results using the second set of boundary conditions of 5% and 3% O_2 in the two reservoirs of the channel slide. For all simulation time points, concentration in the channel had assumed a parabolic shape with peak O_2 concentration at the center of the channel from the 15-35 mm marks with monotonically decreasing values to either the left or the right boundary conditions. At 4 hours, the center of the channel (~25mm mark) was ~18% O_2. As time

went on, O_2 content at the center of the channel ($\sim$25 mm mark) gradually dropped to $\sim$11% and $\sim$7% at 24 and 48 hours, respectively. At each time point, O_2 in the channel sloped monotonically downward from the center ($\sim$25 mm mark) to the edge boundary conditions (at 0 and 50 mm marks).

Next, hydrogels with either 0.2 or 0.4 mg/mL GOX_{PEGA} (20 μL volume) were used within the reservoirs of the channel slide to generate O_2 consumption over time. Shown in Figure 4.15 are measured O_2 values for the use of one or two gels within the reservoirs of the channel slide as well as results of the numerical simulation of the gradient development within the channel.
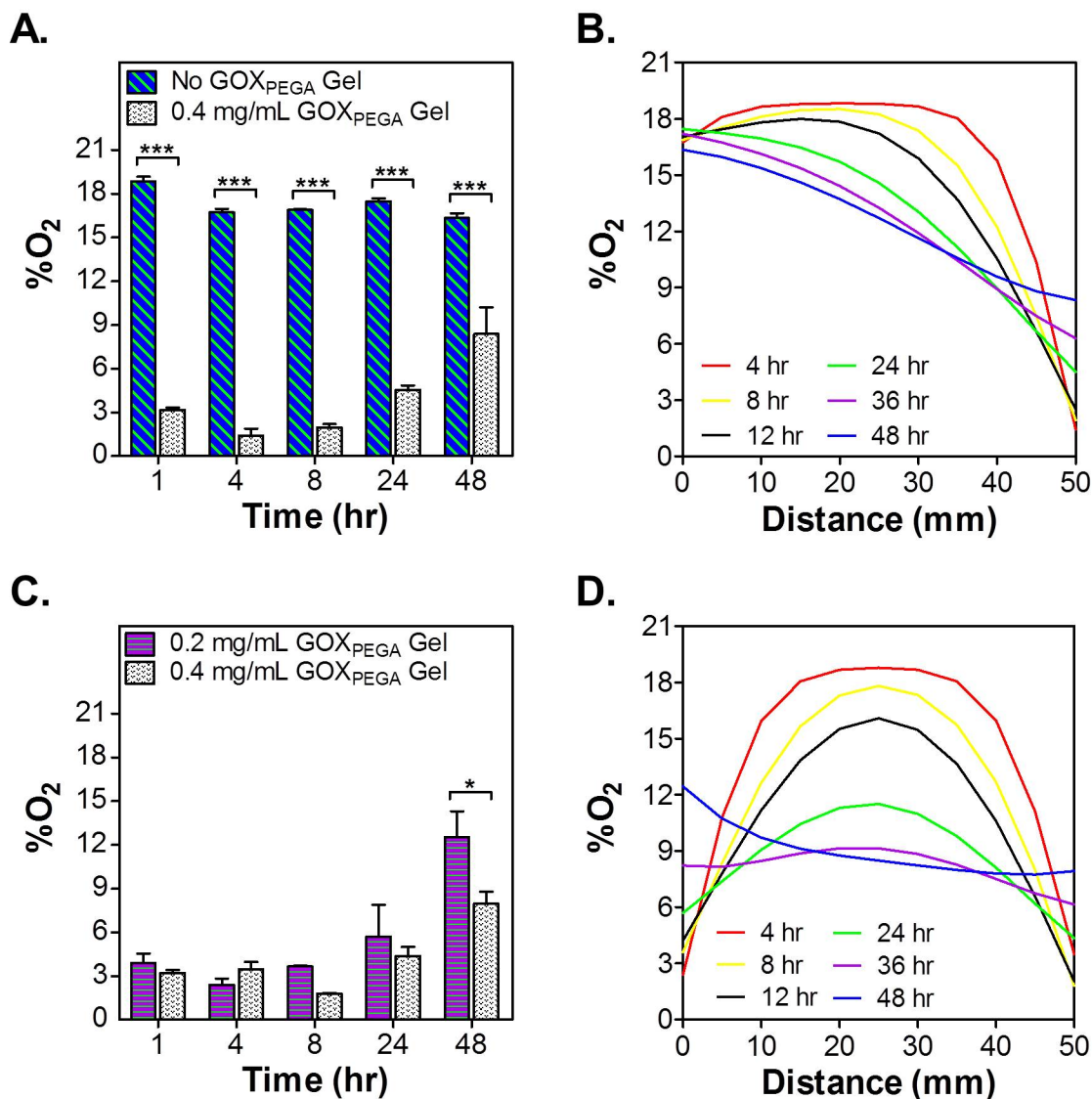
Fig. 4.15. Gradient development using O_2 consuming GOX_{PEGA} Gels in channel plates. (A, C) Percent O_2 measured as a function of time for GOX_{PEGA} hydrogels in an ibidi channel slide. Hydrogels were 20 μL total volume formed by 15 wt% PEGDA and either 0.2 or 0.4 mg/mL GOX_{PEGA} with one gel per channel reservoir. (B, D) Empirical mesh-modeling of Ficks 1D-diffusion equation for O_2 concentration as a function of time and distance across the channel between the reservoirs. Boundary conditions were fixed at the corresponding measured values for gels (A≅B, C≅D). (*p < 0.05. ***p < 0.001. Mean ± SEM, n ≥ 3).

O_2 measurements for channel slides with one reservoir containing a 0.4 mg/mL GOX_{PEGA} gel (no gel in the second reservoir) are shown in Figure 4.15A. O_2 levels

for the no GOX_{PEGA} gel reservoir were near normoxia for all time points (16% to 20% O_2). For the 0.4 mg/mL GOX_{PEGA} gel, O_2 levels initially dropped and were maintained below $\sim$4.5% O_2 for up to 24 hours, and by 48 hours O_2 content had risen slightly to $\sim$8.3%. This result was again consistent with trends seen in other previous cell free measurements shown in Figures 4.8A and 4.9A.

Using the experimentally obtained O_2 data as boundary conditions at opposite ends of the channel (Figure 4.15A), a semi-empirical simulation of O_2 concentration within the channel was developed (Figure 4.15B). Similar to that of Figure 4.14A, at 4 hours of simulated O_2 diffusion within the channel, normoxia (i.e., 17% to 20%) was obtained from the 0-35 mm mark. On the other hand (again at 4 hours), O_2 concentration drops from 18.0% to 1.4% from the 35-50 mm mark. By 12 hours, from the 25-50 mm mark, O_2 concentration monotonically decreased from 17.3% to 2.5%. By 36 hours, from the 10-50 mm marks, O_2 dropped from 17.0% to 4.5%. At 48 hours, the range of the gradient covered the entire channel (from 17.2% (at 0 mm) to 6.3% (at 50 mm)).

For the second case of a channel slide with two gels, Figure 4.15C shows the measured %O_2 over time for reservoirs containing 0.2 mg/mL and 0.4 mg/mL GOX_{PEGA} gels. O_2 levels for both sides within the first 8 hours were fairly similar at $\sim$4%. By 24 and 48 hours, however, the 0.2 mg/mL GOX_{PEGA} gel had started to show higher O_2 tension (from 5% to 13% O_2) compared to the 0.4 mg/mL GOX_{PEGA} gel (from 4% to 8% O_2).

Empirical simulation of O_2 concentration between the wells is shown in Figure 4.15D. The O_2 tension across the channel assumed a parabolic shape, similar to that of Figure 4.14B. Within the first 4 to 36 hours, O_2 concentration within the channel was highest between the 20-30 mm marks (Figure 4.15D). At 4 and 8 hours, O_2 concentration in the channel was predicted to be at $\sim$18% (20-30 mm marks) at the center with decreasing concentration to the far ends of the channel where values were $\sim$3% (0 and 50 mm marks). By 12 hours, using the same locations, the center of the channel (20-30 mm marks) was $\sim$15.5% O_2 with decreasing concentration to either end of the channel at $\sim$3.2% O_2 (0 and 50 mm marks). Then at 24 hours, again

using the same locations, O_2 concentration at the center of the channel was $\sim11.2\%$ dropping to $\sim5.1\%$ at the far ends. However, by 36 hours, O_2 in the channel on the left side was at 8.2% (0 mm mark), while the center was at 9.1% (25 mm mark), and the right side at 6.2% (50 mm mark). After 36 hours, rising O_2 measured in the reservoirs caused an increase in the predicted $\%O_2$ in the channel. At 48 hours, from the 0-30 mm mark, O_2 concentration dropped from $\sim12.5\%$ to 8% while the rest of the channel (30-50 mm mark) was at $\sim8\%$ O_2.

5. SUMMARY & RECOMMENDATIONS

5.1 Summary

This thesis aimed to develop an enabling material strategy to create solution hypoxia for *in vitro* cancer cell culture without using complex devices/instrument. GOX-immobilized hydrogel was used as a proof-of-concept to demonstrate the ability of enzyme-immobilized gel to induce sustained hypoxia. In the first part of this thesis, I established the concentration of GOX (4.5 μg in 1 mL buffer) required to induce hypoxia ($<5\%$) within 5 minutes (Figure 4.1A). As expected, the addition of CAT partially replenished O_2, leading to slight decrease in reaction velocity (Figure 4.1B). Chemical modification is necessary for the immobilization of GOX into hydrogels but significant modification might result in the loss of enzymatic activity, especially when the degree of enzyme modification achieved was more than 90% of the available amine groups on enzyme surface. Analyses of enzyme reaction kinetics revealed that chemical modification (i.e., PEG-acrylation) of GOX only caused slight reduction of its O_2 consumption ability (Figure 4.3B and Table 4.1) [46]. The kinetic parameters of GOX obtained from this study were relatively low compared to values reported in the literature [10]. This could be attributed to the differences in experimental conditions and the methods for which enzyme activities were measured. Conventionally, the activity of GOX is assayed by monitoring β-D-glucose concentration, whereas in the current study O_2 concentration was detected. Although the O_2 contributed from atmospheric air or from reduced H_2O_2 (by CAT or natural reduction with a half-life of $\sim$10 minutes in cell culture environment, [14]) would complicate the analysis results, the current detection method was necessary as the main purpose of this project was to investigate whether enzyme-immobilized hydrogels could induce solution hypoxia for *in vitro* cell culture under ambient conditions (i.e., with O_2 diffusion from the air). The slight reduction of activity in modified enzyme was likely

caused by changes in secondary and tertiary protein structure following significant GOX surface modification [48]. Nonetheless, both unmodified GOX and GOX_{PEGA} were able to induce solution hypoxia ($O_2 < 5\%$) within a few minutes (Figure 4.3A) and solution hypoxia was sustained for up to 24 hours (Figure 4.4). Additionally, no statistically significant difference was observed between GOX and GOX_{PEGA} activity within the first 24 hours (Figure 4.4). Results seen were consistent to that reported by Kang *et al.* where methacryloyl-modified GOX exhibited similar enzymatic activity in solution compared with unmodified GOX [49]. It was also found that GOX_{PEGA} co-polymerized in PEGDA hydrogels was able to induce hypoxia rapidly after dropping the gel in glucose-containing buffer solution. However, GOX-immobilized hydrogel could only sustain solution hypoxia for 24 hours. The restoration of O_2 tension in the solution was not due to lost of enzyme activity as O_2 tension at the interior of the GOX-immobilized hydrogel was maintained below 2% for up to 5 days (Figure 4.7B). It was likely that constant O_2 diffusion from the liquid-air interface supersedes O_2 consuming enzymatic reaction in the hydrogel. This hypothesis was supported by the fact that replacing the old gel with a freshly prepared GOX-immobilized hydrogel only prolonged hypoxia for a few hours (Figure 4.10).

Another possible reason was that some enzymes were deactivated by the accumulation of acid by-product gluconic acid and H_2O_2. To test whether H_2O_2 deactivated the enzyme, CAT was introduced in the solution to consume H_2O_2 (Figure 4.8). The increase of O_2 content in the solution (Figure 4.8A) coincided with the accumulation of H_2O_2 levels (Figure 4.8B), supporting the likelihood of enzyme deactivation by elevated H_2O_2 concentration. This phenomenon has been reported in membrane-bound GOX and CAT system where both enzyme activities were reduced with increased H_2O_2 concentrations over time [22,50]. It was not likely that the enzymatic reactions depleted most of the substrate (i.e., β-D-glucose) after 24 hours, as the addition of extra β-D-glucose periodically before O_2 tension measurement did not cause further O_2 consumption. Whether there was additional glucose addition or not, no statistically significant difference was found in O_2 (Figure 4.9A) or H_2O_2 concentration (Figure 4.9B).

For the second part of this thesis, the utility of the immobilized enzyme system for *in vitro* cell culture was demonstrated. Cell viability, proliferation, and the expression of hypoxia-regulated genes (i.e., CA9 or LOX) in cells cultured in the presence of GOX-immobilized hydrogels were characterized. Both CA9 and LOX are downstream targets of HIF1α and are well-established genes associated with cancer metastasis and metabolism in hypoxic environments [51, 52]. Detecting the expression of these two genes allowed evaluation of the utility of the hypoxia-inducing hydrogels [46]. Results show that the expression of CA9 and LOX was significantly higher in Huh7 cells cultured with GOX-immobilized hydrogels (Figures 4.12D & 4.13). Molm14 cells also had increased CA9 expression (Figure 4.12B). However, no expression of LOX was detected (control group included); there is also a lack of literature for LOX expression with Molm14 cells or the sister Molm13 cell line. Nonetheless, similar data for both CA9 and LOX expression was reported by Askoxylakis *et al.* where GOX and CAT were dissolved in culture media to generate hypoxia for culturing head and neck squamous carcinoma cells [15].

Hypoxic response in the cells can also be simulated using chemicals that upregulate or stabilize the expression of HIF, specifically HIF1α. Cobalt chloride ($CoCl_2$) or desferrioxamine are two examples of such chemicals [53]. Although this is a relatively simple strategy to mimic hypoxic response in the cells, the use of chemical only regulates cellular and molecular responses directly downstream of HIF. Furthermore, these chemicals could affect cell survival, metabolism, and morphology differently compared to real O_2 deprivation [54]. Regardless of this, $CoCl_2$ is often used as a standard chemical means to induce hypoxic gene response in cells rather than an incubator with prescribed O_2 levels. Figures 4.12D and 4.13 both indicated that the GOX_{PEGA} hydrogels with CAT were faster at inducing hypoxic gene response as well as able to induce a higher fold change versus that of $CoCl_2$. Although GOX-immobilized hydrogel was effective in inducing solution hypoxia under ambient conditions, these gels appeared to hinder cell viability and proliferation after the cells were exposed to the hydrogel system for longer than 24 hours. This was most likely attributed to the accumulation of cytotoxic byproduct, namely gluconic acid and H_2O_2. This is not a

unique problem to my system as other GOX/CAT-induced hypoxia culture systems (e.g., soluble or membrane-bound enzyme) also exhibited decreased cytocompatibility after 24 hours of culture [15, 16, 19]. One potential solution for this drawback is to replace the GOX-immobilized hydrogel and the CAT supplemented media frequently. Providing fresh media and hydrogel allows hypoxia to quickly be reestablished and maintained for periods lasting for at least 24 hours. Furthermore, media acidification by gluconic acid could be reduced by supplementing cell culture media with HEPES, which provides strong buffering effect without altering normal cell physiology.

Finally, for the third part of this thesis, channel slides were used in conjunction with GOX_{PEGA} gels to create hypoxia gradient (Figure 4.15). Owing to the geometry of the slide itself, O_2 concentration was only measured at the actual entrance to the channel on either side within the reservoirs ($\sim$1 mm directly above GOX_{PEGA} gels). By using a gel in one or both reservoirs in the channel, hypoxia was created at one or both ends of the channel slide. Data generated for the O_2 tension (Figure 4.15A & C) was very similar to that of previous cell free measurements in that for reservoirs with gels, O_2 tension was $\sim$5% or less within the first 24 hours and by 48 hours had risen to more than 10%. From the data generated in the reservoirs of the channel slides, a mathematical model was applied to semi-empirically predict the O_2 within the channel over time (Figure 4.15B & D). In the first scenario, where one reservoir was empty and the other reservoir had a gel, a monotonically decreasing gradient of O_2 developed across the width of the channel from 24 to 48 hours (Figure 4.15A & B). In the second scenario where one gel was placed in each reservoir, simulation results show bimodal O_2 gradients developed within the first 12 hours in the channel (4.15C & D). In other words, O_2 concentration was highest at the center (20-30 mm) with decreasing concentration to the left and right far ends of the channel (0 and 50 mm).

In summary, immobilized GOX was used to induce O_2 tension at less than 10% O_2 in solution for up to 24 hours. Secondly, the effect of hypoxia induced by the dual enzymes (i.e., immobilized GOX and soluble CAT) on cell culture was studied and found to be cytocompatible for at least 24 hours. Hypoxia induced by GOX-immobilized

hydrogels led to increased expression of hypoxia associated genes CA9 and LOX. Lastly, immobilized GOX gels were used to induce hypoxia gradients within specialized channel slides. Semi-empirical mathematical modeling predicted that monotonic decreasing (only one GOX-immobilized gel placed in a reservoir) and bimodal (GOX-immobilized gels placed in both reservoirs) gradients existed within the channel slides during specific windows of time over the course of the experiment.

5.2   Recommendations

Future work will focus on expanding the window of hypoxia induced by the enzyme-immobilized hydrogels. With the current GOX/CAT system, a simple method for prolonged hypoxia would be to supplement with fresh enzyme. Additionally, GOX/CAT induced hypoxia could also be expanded through the stabilization of the enzymes from the H_2O_2 and gluconic acid being produced. Simple buffering chemicals like HEPES or glutathione can be used to neutralize the reaction byproducts. Excipients (stabilizing molecules) represent a second method to stabilize the GOX/CAT enzymes. Two such stabilizers, trehalose, a non-reducing disaccharide, and silk fibroin, a purified protein structure from cocoons of silk worms, have been known to enhance long term functional activity of enzymes in hydrogels [55, 56].

A second avenue of future work should focus on alternative O_2-consuming enzymes which do not produce enzyme-damaging (and often cytotoxic) byproducts like H_2O_2 and gluconic acid. Examples of O_2 consuming enzymes in this category are laccase, bilirubin oxidase, polyphenol oxidase, and catechol oxidase to name a few. Additionally, different enzymatic reaction speeds would create different levels of hypoxia induction within a given time frame.

Finally, future studies should expand the use of enzyme-immobilized hydrogels for hypoxic gradient creation. Cancer cell lines can be cultured with O_2-consuming immobilized-enzyme hydrogels within a channel slide. Using the semi-empirical modeling, experimental time frames could be determined as to when it is appropriate to investigate possible O_2 gradient induced cellular migration in the channel slides.

LIST OF REFERENCES

LIST OF REFERENCES

[1] M. C. Simon and B. Keith, "The role of oxygen availability in embryonic development and stem cell function," *Nat Rev Mol Cell Biol*, vol. 9, no. 4, pp. 285–96, 2008.

[2] M. P. De Miguel, Y. Alcaina, D. S. de la Maza, and P. Lopez-Iglesias, "Cell metabolism under microenvironmental low oxygen tension levels in stemness, proliferation and pluripotency," *Curr Mol Med*, vol. 15, no. 4, pp. 343–59, 2015.

[3] G. L. Semenza, "Hif-1: mediator of physiological and pathophysiological responses to hypoxia," *J Appl Physiol (1985)*, vol. 88, no. 4, pp. 1474–80, 2000.

[4] M. Hockel and P. Vaupel, "Tumor hypoxia: definitions and current clinical, biologic, and molecular aspects," *J Natl Cancer Inst*, vol. 93, no. 4, pp. 266–76, 2001.

[5] L. Liu and M. C. Simon, "Regulation of transcription and translation by hypoxia," *Cancer Biol Ther*, vol. 3, no. 6, pp. 492–7, 2004.

[6] A. Giaccia, B. G. Siim, and R. S. Johnson, "Hif-1 as a target for drug development," *Nat Rev Drug Discov*, vol. 2, no. 10, pp. 803–11, 2003.

[7] C. B. Allen, B. K. Schneider, and C. W. White, "Limitations to oxygen diffusion and equilibration in in vitro cell exposure systems in hyperoxia and hypoxia," *Am J Physiol Lung Cell Mol Physiol*, vol. 281, no. 4, pp. L1021–7, 2001.

[8] H. E. Broxmeyer, H. A. O'Leary, X. Huang, and C. Mantel, "The importance of hypoxia and extra physiologic oxygen shock/stress for collection and processing of stem and progenitor cells to understand true physiology/pathology of these cells ex vivo," *Current opinion in hematology*, vol. 22, no. 4, pp. 273–278, 2015.

[9] C. C. Peng, W. H. Liao, Y. H. Chen, C. Y. Wu, and Y. C. Tung, "A microfluidic cell culture array with various oxygen tensions," *Lab Chip*, vol. 13, no. 16, pp. 3239–45, 2013.

[10] Q. H. Gibson, B. E. Swoboda, and V. Massey, "Kinetics and mechanism of action of glucose oxidase," *J Biol Chem*, vol. 239, pp. 3927–34, 1964.

[11] H. N. Kirkman and G. F. Gaetani, "Mammalian catalase: a venerable enzyme with new mysteries," *Trends Biochem Sci*, vol. 32, no. 1, pp. 44–50, 2007.

[12] R. P. Baumann, P. G. Penketh, H. A. Seow, K. Shyam, and A. C. Sartorelli, "Generation of oxygen deficiency in cell culture using a two-enzyme system to evaluate agents targeting hypoxic tumor cells," *Radiat Res*, vol. 170, no. 5, pp. 651–60, 2008.

[13] G. Millonig, S. Hegedusch, L. Becker, H. K. Seitz, D. Schuppan, and S. Mueller, "Hypoxia-inducible factor 1 alpha under rapid enzymatic hypoxia: cells sense decrements of oxygen but not hypoxia per se," *Free Radic Biol Med*, vol. 46, no. 2, pp. 182–91, 2009.

[14] S. Mueller, G. Millonig, and G. N. Waite, "The gox/cat system: a novel enzymatic method to independently control hydrogen peroxide and hypoxia in cell culture," *Adv Med Sci*, vol. 54, no. 2, pp. 121–35, 2009.

[15] V. Askoxylakis, G. Millonig, U. Wirkner, C. Schwager, S. Rana, A. Altmann, U. Haberkorn, J. Debus, S. Mueller, and P. E. Huber, "Investigation of tumor hypoxia using a two-enzyme system for in vitro generation of oxygen deficiency," *Radiat Oncol*, vol. 6, p. 35, 2011.

[16] K. Zitta, P. Meybohm, B. Bein, Y. Huang, C. Heinrich, J. Scholz, M. Steinfath, and M. Albrecht, "Salicylic acid induces apoptosis in colon carcinoma cells grown in-vitro: influence of oxygen and salicylic acid concentration," *Exp Cell Res*, vol. 318, no. 7, pp. 828–34, 2012.

[17] N. Rajan, A. Narayan, Z. Wu, P. Wu, C. H. Ahn, R. K. Narayan, and C. Li, "A novel oxygen tension programmable microfluidic system (oproms) for in vitro cell biology studies," *2013 Transducers and Eurosensors XXVII: The 17th International Conference on Solid-State Sensors, Actuators and Microsystems*, pp. 412–415, 2013.

[18] M. C. Sobotta, A. G. Barata, U. Schmidt, S. Mueller, G. Millonig, and T. P. Dick, "Exposing cells to h2o2: a quantitative comparison between continuous low-dose and one-time high-dose treatments," *Free Radic Biol Med*, vol. 60, pp. 325–35, 2013.

[19] Y. Huang, K. Zitta, B. Bein, M. Steinfath, and M. Albrecht, "An insert-based enzymatic cell culture system to rapidly and reversibly induce hypoxia: investigations of hypoxia-induced cell damage, protein expression and phosphorylation in neuronal imr-32 cells," *Dis Model Mech*, vol. 6, no. 6, pp. 1507–14, 2013.

[20] C. Li, W. Chaung, C. Mozayan, R. Chabra, P. Wang, and R. K. Narayan, "A new approach for on-demand generation of various oxygen tensions for in vitro hypoxia models," *PLoS One*, vol. 11, no. 5, p. e0155921, 2016.

[21] J. P. Fruehauf and J. Meyskens, F. L., "Reactive oxygen species: a breath of life or death?" *Clin Cancer Res*, vol. 13, no. 3, pp. 789–94, 2007.

[22] P. H. Tse and D. A. Gough, "Time-dependent inactivation of immobilized glucose oxidase and catalase," *Biotechnol Bioeng*, vol. 29, no. 6, pp. 705–13, 1987.

[23] P. Pal, S. Datta, and P. Bhattacharya, "Studies on the modeling and simulation of a sequential bienzymatic reaction system immobilized in emulsion liquid membrane," *Biochem Eng J*, vol. 5, no. 2, pp. 89–100, 2000.

[24] A. Hielscher and S. Gerecht, "Hypoxia and free radicals: role in tumor progression and the use of engineering-based platforms to address these relationships," *Free Radic Biol Med*, vol. 79, pp. 281–91, 2015.

[25] D. Trachootham, J. Alexandre, and P. Huang, "Targeting cancer cells by ros-mediated mechanisms: a radical therapeutic approach?" *Nat Rev Drug Discov*, vol. 8, no. 7, pp. 579–91, 2009.

[26] Q. Wu, L. Wang, H. Yu, J. Wang, and Z. Chen, "Organization of glucose-responsive systems and their properties," *Chem Rev*, vol. 111, no. 12, pp. 7855–75, 2011.

[27] D. Choi, W. Lee, J. Park, and W. Koh, "Preparation of poly(ethylene glycol) hydrogels with different network structures for the application of enzyme immobilization," *Biomed Mater Eng*, vol. 18, no. 6, pp. 345–56, 2008.

[28] M. Blatchley, K. M. Park, and S. Gerecht, "Designer hydrogels for precision control of oxygen tension and mechanical properties," *J Mater Chem B Mater Biol Med*, vol. 3, no. 40, pp. 7939–7949, 2015.

[29] K. M. Park, M. R. Blatchley, and S. Gerecht, "The design of dextran-based hypoxia-inducible hydrogels via in situ oxygen-consuming reaction," *Macromol Rapid Commun*, vol. 35, no. 22, pp. 1968–75, 2014.

[30] K. M. Park and S. Gerecht, "Hypoxia-inducible hydrogels," *Nat Commun*, vol. 5, p. 4075, 2014.

[31] D. M. Lewis, K. M. Park, V. Tang, Y. Xu, K. Pak, T. S. Eisinger-Mathason, M. C. Simon, and S. Gerecht, "Intratumoral oxygen gradients mediate sarcoma cell invasion," *Proc Natl Acad Sci U S A*, vol. 113, no. 33, pp. 9292–7, 2016.

[32] C.-C. Lin, "Recent advances in crosslinking chemistry of biomimetic poly (ethylene glycol) hydrogels," *RSC advances*, vol. 5, no. 50, pp. 39 844–39 853, 2015.

[33] M. A. Azagarsamy and K. S. Anseth, "Bioorthogonal click chemistry: An indispensable tool to create multifaceted cell culture scaffolds," *ACS Macro Letters*, vol. 2, no. 1, pp. 5–9, 2013.

[34] C.-C. Lin and K. S. Anseth, "Cellcell communication mimicry with poly (ethylene glycol) hydrogels for enhancing β-cell function," *Proceddings of the National Academy of Sciences*, vol. 108, no. 16, pp. 6380–6385, 2011.

[35] L. H. Gray, A. Conger, M. Ebert, S. Hornsey, and O. Scott, "The concentration of oxygen dissolved in tissues at the time of irradiation as a factor in radiotherapy," *The British journal of radiology*, vol. 26, no. 312, pp. 638–648, 1953.

[36] P. Vaupel, A. Mayer, and M. Hckel, "Tumor hypoxia and malignant progression," *Methods in enzymology*, pp. 335–354, 2004.

[37] P. Vaupel, "Prognostic potential of the pretherapeutic tumor oxygenation status," *Oxygen Transport to Tissue XXX*, pp. 241–246, 2009.

[38] D. M. Gilkes, G. L. Semenza, and D. Wirtz, "Hypoxia and the extracellular matrix: drivers of tumour metastasis," *Nature Reviews Cancer*, vol. 14, no. 6, pp. 430–439, 2014.

[39] D. R. Grimes, C. Kelly, K. Bloch, and M. Partridge, "A method for estimating the oxygen consumption rate in multicellular tumour spheroids," *Journal of The Royal Society Interface*, vol. 11, no. 92, p. 20131124, 2014.

[40] J. T. Erler, K. L. Bennewith, M. Nicolau, N. Dornhfer, C. Kong, Q.-T. Le, J.-T. A. Chi, S. S. Jeffrey, and A. J. Giaccia, "Lysyl oxidase is essential for hypoxia-induced metastasis," *Nature*, vol. 440, no. 7088, pp. 1222–1226, 2006.

[41] T. R. Cox, D. Bird, A.-M. Baker, H. E. Barker, M. W. Ho, G. Lang, and J. T. Erler, "Lox-mediated collagen crosslinking is responsible for fibrosis-enhanced metastasis," *Cancer research*, vol. 73, no. 6, pp. 1721–1732, 2013.

[42] C. G. Colpaert, P. B. Vermeulen, S. B. Fox, A. L. Harris, L. Y. Dirix, and E. A. Van Marck, "The presence of a fibrotic focus in invasive breast carcinoma correlates with the expression of carbonic anhydrase ix and is a marker of hypoxia and poor prognosis," *Breast cancer research and treatment*, vol. 81, no. 2, pp. 137–147, 2003.

[43] C. Trastour, E. Benizri, F. Ettore, A. Ramaioli, E. Chamorey, J. Pouyssgur, and E. Berra, "Hif1 and ca ix staining in invasive breast carcinomas: Prognosis and treatment outcome," *International journal of cancer*, vol. 120, no. 7, pp. 1451–1458, 2007.

[44] Y. Hao and C. C. Lin, "Degradable thiol-acrylate hydrogels as tunable matrices for three-dimensional hepatic culture," *J Biomed Mater Res A*, vol. 102, no. 11, pp. 3813–27, 2014.

[45] B. D. Fairbanks, M. P. Schwartz, C. N. Bowman, and K. S. Anseth, "Photoinitiated polymerization of peg-diacrylate with lithium phenyl-2,4,6-trimethylbenzoylphosphinate: polymerization rate and cytocompatibility," *Biomaterials*, vol. 30, no. 35, pp. 6702–7, 2009.

[46] C. S. Dawes, H. Konig, and C.-C. Lin, "Enzyme-immobilized hydrogels to create hypoxia for in vitro cancer cell culture," *Journal of Biotechnology*, vol. 248, pp. 25–34.

[47] S. Cahpra and R. Canale, "Numerical methods for engineers 5th," 2006.

[48] P. Pandey, S. P. Singh, S. K. Arya, V. Gupta, M. Datta, S. Singh, and B. D. Malhotra, "Application of thiolated gold nanoparticles for the enhancement of glucose oxidase activity," *Langmuir*, vol. 23, no. 6, pp. 3333–7, 2007.

[49] S. I. Kang and Y. H. Bae, "A sulfonamide based glucose-responsive hydrogel with covalently immobilized glucose oxidase and catalase," *Journal of Controlled Release*, vol. 86, no. 1, pp. 115–121, 2003.

[50] A. Blandino, M. Macas, and D. Cantero, "Modelling and simulation of a bienzymatic reaction system co-immobilised within hydrogel-membrane liquid-core capsules," *Enzyme and microbial technology*, vol. 31, no. 4, pp. 556–565, 2002.

[51] C. C. Wykoff, N. J. P. Beasley, P. H. Watson, K. J. Turner, J. Pastorek, A. Sibtain, G. D. Wilson, H. Turley, K. L. Talks, P. H. Maxwell, C. W. Pugh, P. J. Ratcliffe, and A. L. Harris, "Hypoxia-inducible expression of tumor-associated carbonic anhydrases," *Cancer Research*, vol. 60, no. 24, pp. 7075–7083, 2000.

[52] J. T. Erler, K. L. Bennewith, M. Nicolau, N. Dornhofer, C. Kong, Q.-T. Le, J.-T. A. Chi, S. S. Jeffrey, and A. J. Giaccia, "Lysyl oxidase is essential for hypoxia-induced metastasis," *Nature*, vol. 440, no. 7088, pp. 1222–1226, 2006.

[53] W. G. An, M. Kanekal, M. C. Simon, E. Maltepe, M. V. Blagosklonny, and L. M. Neckers, "Stabilization of wild-type p53 by hypoxia-inducible factor 1alpha," *Nature*, vol. 392, no. 6674, pp. 405–8, 1998.

[54] Y. H. Han, L. Xia, L. P. Song, Y. Zheng, W. L. Chen, L. Zhang, Y. Huang, G. Q. Chen, and L. S. Wang, "Comparative proteomic analysis of hypoxia-treated and untreated human leukemic u937 cells," *Proteomics*, vol. 6, no. 11, pp. 3262–74, 2006.

[55] T. M. O'shea, M. J. Webber, A. A. Aimetti, and R. Langer, "Covalent incorporation of trehalose within hydrogels for enhanced longterm functional stability and controlled release of biomacromolecules," *Advanced healthcare materials*, vol. 4, no. 12, pp. 1802–1812, 2015.

[56] E. M. Pritchard, P. B. Dennis, F. Omenetto, R. R. Naik, and D. L. Kaplan, "Physical and chemical aspects of stabilization of compounds in silk," *Biopolymers*, vol. 97, no. 6, pp. 479–498, 2012.
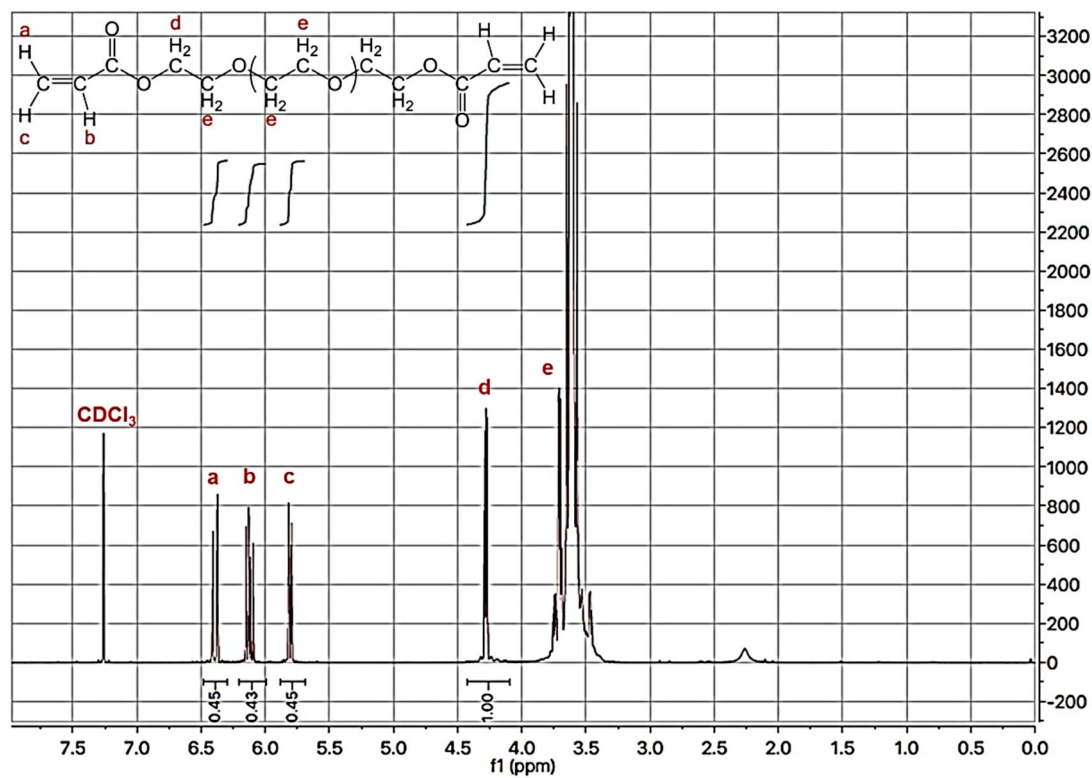
APPENDIX

A. APPENDIX

A.1 PEGDA ¹H-NMR

Fig. A.1. ¹H-NMR spectra of PEGDA. The degree of acrylation was calculated by comparing the ratio of the integrals of the acrylate group (a-b-c, $\delta 5.8 - 6.4$ ppm) to the terminal -CH$_2$ of the PEG backbone (d, $\delta 4.3$ ppm).

A.2 RT-PCR Gene Sequences

Table A.1. Gene sequences used for Real time PCR.

Gene	Sequence	Reference
18S	f: ATCCCTGAAAAGTTCCAGCA	Pombo-Suarez M, et al.
	r: CCCTCTTGGTGAGGTCAATG	*BMC Mol Biol.* 2008;9:17.
HIF1α	f: GAACGTCGAAAAGAAAAGTCTCG	
	r: CCTTATCAAGATGCGAACTCACA	Designed with
LOX	f: CGGCGGAGGAAAACTGTCT	Harvard Primer Bank,
	r: TCGGCTGGGTAAGAAATCTGA	pga.mgh.harvard.edu
CA9	f: GGATCTACCTACTGTTGAGGCT	/primerbank/
	r: CATAGCGCCAATGACTCTGGT	

A.3 Preliminary Study: Effect of Lyophilization on GOX_{PEGA} Gel Induced Hypoxia

Lyophilization of the hydrogels was done to provide convenience of use of the gels at a later date post synthesis. The gels are simply frozen and then thawed/rehydrated at a later date for O_2 tension measurements. Shown in Figure A.2 is the O_2 tension development over time within the ibidi channel slide for gels used immediately after synthesis and swelling (Figure A.2A) versus gels that were synthesized, lyophilized and then allowed to swell (Figure A.2B):
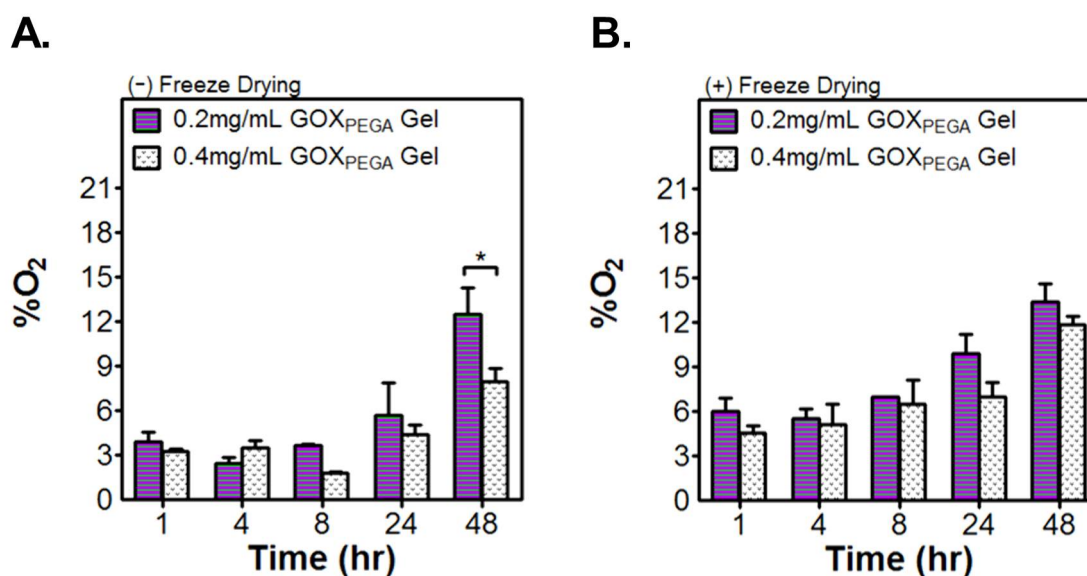

Fig. A.2. Effect of lyophilization on O_2 consumption by GOX_{PEGA} gels. O_2 tension over time for GOX_{PEGA} gels with (B) and without (A) lyophilization. Hydrogels (20 μL) were formed by 15 wt% PEGDA and 0.2 or 0.4 mg/mL GOX_{PEGA} with one gel per reservoir in the ibidi channel slide. All gels were added to 37°C DPBS for swelling overnight before use. (*p < 0.05. Mean ± SEM, n ≥ 3).

In general, O_2 contents were higher for gels that were lyophilized compared to gels that were used without lyophilization. For the 0.2 mg/mL gels in Figure A.2A and A.2B, average difference between the two groups was around 1 4% O_2 for all time points. The 0.4 mg/mL gels in Figure A.2A and A.2B also showed a similar

average difference between the two groups of 1   5% O_2 for all time points. The average difference of measured O_2 between the two gel groups in Figure A.2A (without lyophilization) was not found to be statistically different from the average difference of measured O_2 between the two gel groups in Figure A.2B (with lyophilization). It is of note that Figure A.2A is a reproduction of Figure 4.15C.

A.4 Semi-Empirical Prediction of O_2 Gradient Development in Channel Slides

Matlab Code A.1: Finite Difference Calculations for One Dimensional Diffusion

```matlab
1  clear all; close all; clc; format long;
2  sr=['b   ';'r   ';'g   ';'m   '];
3  sr2=['bo  ';'ro  ';'go  ';'mo  '];
4  sr3=['kd  ';'kd  ';'kd  ';'kd  '];
5
6  %%%%
7  % experimental data and corresponding time points
8  t=[1 4 8 24 48]';
9  o2_data=[18.8068 3.4855 19.411 2.9783 18.2602 2.987
10         3.2735 2.966 5.1629 3.6655 3.2735 2.966;
11          17.1425 2.2609 16.3297 1.3149 16.6893 0.647
12          2.831 3.9618 1.501 2.4866 2.831 3.9618;
13          16.9636 1.8467 16.8536 1.6158 16.8278 2.4214
14          3.5878 1.8321 3.7652 1.6929 3.5878 1.8321;
15          17.1678 4.1648 17.3821 4.3081 17.8364 5.1629
16          3.5404 3.7553 10.0435 5.6274 3.5404 3.7553;
17          16.4299 11.9364 15.7061 7.2729 16.8423 5.929
18          11.5356 9.0345 15.9684 8.5443 10.0909 6.3022];
19  [m,n]=size(o2_data);
20
21  %%%%
22  % generating more time points for hermite splines
23  % p_t=linspace(min(t),max(t),40); %doesn't change sem later to ...
       plot more
24  p_t=1:0.25:48; %doesn't change sem later to plot more
25
26  % calculating the average increment of time (used for the mesh later)
27  counter=1;
28  for count=length(t):-1:2
29      del_t(counter)=p_t(count)-p_t(count-1);
```

```matlab
30      counter=counter+1;
31  end
32  del_t=mean(del_t); %hr
33
34  %%%%
35  % generating hermite splines between each data point for each well
36  % (represented by columns above)
37  for count=1:1:n
38      s_o2_data(:,count)=pchip(t,o2_data(:,count),p_t);
39  end
40
41  %%%%
42  % parameters for mesh from centered
43  % finite-divided-difference approximation of the 1D
44  % Diffusion equation with respect to time and distance
45
46  % Oxygen concentration in solution without any enzyme added (Co)
47  normal_o2_set=18.826;
48
49  % mesh distance span and increment
50  del_x=5; %mm
51  Length=50; %mm
52  x=[0:del_x:Length]';
53
54  % diffusivity of oxygen
55  Da=2.7*(10^-9); %oxygen in 37dC water, meter squared per second
56
57  % mesh multiplication factor
58  lambda=Da*(del_t/(del_x^2))*1000*1000*60*60;
59
60  %%%%
61  % generating the mesh matrix, columns from left to right represent
62  % increasing distance (starting with zero), rows from top to bottom
63  % represent timepoints (starting with zero)
64  for count=2:2:n
65  %     aside=s_o2_data(:,count-1);
```

```
66  %     bside=s_o2_data(:,count);

67

68      aside=normal_o2_set*ones(size(s_o2_data(:,count-1)));

69      bside=3*ones(size(s_o2_data(:,count)));

70

71      % filling mesh with initial values

72      % on side A (left) and B (right)

73      O2_mesh=[normal_o2_set*ones(1,Length/del_x+1);

74      aside,zeros(length(aside),Length/del_x-1),bside];

75      [m,n]=size(O2_mesh);

76

77      % filling the mesh with the central difference values

78      for L=1:1:m-1 %row

79          for I=2:1:n-1 %column

80              O2_mesh(L+1,I)=O2_mesh(L,I)

81              +lambda*(O2_mesh(L,I+1)

82              -2*O2_mesh(L,I)+O2_mesh(L,I-1));

83          end

84      end

85

86      % summary cell of each mesh generated

87      all_ans{count/2}=O2_mesh;

88  end

89

90

91      index=[4,8,12,24,36,48];

92  for counting=1:1:length(index)

93  indexer(counting)=find(p_t==index(counting));

94  end

95

96

97  %%%%

98  % group representation (average and sem),

99  % data generated in this loop is

100 % taken to be plotted in GraphPad Prism

101 for count=3:3:6
```

```matlab
102     a=cell2mat(all_ans(count-2));
103     b=cell2mat(all_ans(count-1));
104     c=cell2mat(all_ans(count-0));
105     mesh_avg=(a+b+c)/3; %average of the mesh replicates
106
107     for counting=1:1:length(indexer)
108         prism_mesh_format(:,counting)=
109         mesh_avg(indexer(counting),:)';
110     end
111
112 %       %[time, mesh_o2_distances(avg, sem, n)]
113     mesh_val_prism{count/3}=[x,prism_mesh_format];
114 end
```